PROGRESS TOWARDS THE STRUCTURAL BASIS OF TEC-FAMILY KINASE ACTIVATION BY HIV-1 NEF

By

Kindra N. Whitlatch

BS, West Virginia Wesleyan College, 2013

Submitted to the Graduate Faculty of

School of Medicine in partial fulfillment

of the requirements for the degree of

Master of Science

University of Pittsburgh

2018

UNIVERITY OF PITTSBURGH

SCHOOL OF MEDICINE

This thesis was presented

by

Kindra N. Whitlatch

It was defended on

August 17, 2018

and approved by

Rieko Ishima, Associate Professor, Department of Structural Biology

John Jeff Alvarado, Research Assistant Professor, Department of Microbiology and Molecular Genetics

Thesis Advisor: Thomas E. Smithgall, William S. McEllroy Professor and Chair, Department of Microbiology and Molecular Genetics

PROGRESS TOWARDS THE STRUCTURAL BASIS OF TEC-FAMILY KINASE ACTIVATION BY HIV-1 NEF

Kindra N. Whitlatch, M.S.

University of Pittsburgh, 2018

HIV-1 Nef is a viral accessory factor that is essential for virus infectivity, host immune evasion and AIDS progression. Nef lacks intrinsic catalytic activity and functions instead via interactions with multiple classes of host cell proteins involved in signal transduction and endocytic trafficking. Nef interacts with the Src-family tyrosine kinases Hck and Lyn through their SH3 domains, resulting in constitutive kinase activity. Nef also binds to select members of the Tec-family of tyrosine kinases, including Btk, Bmx, and Itk, all of which are expressed in HIV-1 target cells. Of particular interest is Itk, which is expressed in $CD4^+$ T cells and is activated by Nef. Selective Itk inhibitors block Nef-dependent enhancement of HIV-1 infectivity and replication, suggesting an important role in the viral life cycle. While the interaction between Itk and Nef has been demonstrated at the plasma membrane in cell-based fluorescence complementation assays, the structural basis of this interaction has not been reported. Like Src-family kinases, Itk has a core region consisting of sequential SH3, SH2 and kinase domains. In addition, Itk has an N-terminal pleckstrin homology (PH) domain important for membrane targeting as well as a Tec homology

(TH) region involved in kinase regulation. To explore the structure of the Nef:Tec-family kinase (TFK) complexes, I have created a panel of bacterial expression constructs for the Itk and Btk regulatory region. These include the entire PH-TH-SH3-SH2 region, the SH3-SH2 region, and the isolated SH3 domain, all of which have yielded mg amounts of soluble protein. I have also produced recombinant, N-terminally myristoylated (Myr) Nef in bacteria, a post-translational modification essential for Nef membrane localization in cells. Preliminary Surface Plasmon Resonance (SPR) studies show that Myr-Nef binds membrane bilayers with low μM affinity in a Myr-dependent manner. These proteins will provide the foundation for future structural determination of Nef-TFK complexes by X-ray crystallography as well as the nature of this interaction in lipid bilayers, the physiological site of interaction in HIV-infected cells.

TABLE OF CONTENTS

LIST OF TABLES

LIST OF FIGURES

ACKNOWLEDGEMENTS

I would like to convey my appreciation and gratitude to my primary thesis advisor, Tom Smithgall, for all the support he has shown me over the years as I have worked and studied in his laboratory. Tom has been an extremely supportive and a kind, competent mentor throughout my graduate career. I would also like to thank all the members of the Smithgall lab, in particular Drs. John Jeff Alvarado and Lori Emert-Sedlak, for their invaluable guidance in lab and in life over the last five years. Their unending support and humor have been an integral piece of my time at the University of Pittsburgh, and I cannot honestly imagine the previous phase of my life without their help and encouragement.

I would also like to thank the Molecular Biophysics and Structural Biology graduate program faculty and staff for their continued assistance throughout the time I have spent at Pitt. I'd similarly like to acknowledge the aid I have received from the other members of my thesis committee in the form of scientific and emotional encouragement; thank you Patrick and Rieko for always being available for a chat if I needed it.

Finally, I'd like to thank my friends and family as they have stood by my side as I have made many changes to my life and plans over the past few years. I would not have made it to this point in my career without their backing and support. I can never overstate the importance of those individuals who have offered their time and support to help me further my education.

1.0 INTRODUCTION

1.1 HIV-1 NEF IN VIRAL PATHOGENESIS AND AIDS

Infection with the human immunodeficiency virus (HIV-1) results in severe immunodeficiency brought about by the chronic depletion of CD4+ T lymphocytes (1), leading to the Acquired Immunodeficiency Syndrome (AIDS). The HIV/AIDS global pandemic is responsible for over 25 million AIDS-related deaths in the last 30 years, with 33 million people presently infected with the virus (2). The introduction of antiretroviral drugs that target critical enzymes in the HIV-1 viral life cycle and fusion to the host cell have dramatically affected the life span of HIV positive individuals. However, HIV is not cleared from the patients, and the chronic condition must be controlled with persistent administration of antiretroviral therapy (2, 3). This chronic therapy, along with the mutational frequency of HIV, has fueled the establishment of multi-drug resistant strains of HIV-1. Along with ambiguous chances for an effective vaccine (4), these drug resistant strains of HIV-1 highlight the need for antiretroviral treatments with complementary mechanisms and targets to the existing therapies.

The HIV-1 genome encodes the retroviral genes Gag, Pol, and Env, as well as proteins that regulate RNA splicing (Rev) and viral transcription (Tat). The current protein targets for HIV-1 treatments – reverse transcriptase, integrase, protease, and the gp41 envelope glycoprotein – are products of the Pol and Env genes (2, 3). Four distinctive accessory proteins are also encoded by HIV-1: Nef, Vif, Vpu, and Vpr. These accessory proteins promote viral growth and pathogenesis and represent alternative antiretroviral targets for future therapies (5). HIV-1 Nef, in particular, is a promising target as a large body of evidence supports a critical role for Nef in HIV-1 pathogenesis. In an early study utilizing a rhesus macaque animal model, infection with an SIV (simian immunodeficiency virus) variant lacking *nef* sequences did not result in sAIDS, indicating that Nef is essential for the progression from SIV infection into AIDS-like disease (6). Conversely, in a transgenic mouse model, the expression of Nef alone is sufficient to drive HIV pathogenesis (7), producing an immunodeficiency syndrome that includes loss of CD4+ T lymphocytes reminiscent of HIV infection in humans. Interestingly, some patients who carry HIV-1 variants that are defective in *nef* sequences are described as long-term non-progressors, meaning their HIV infections persist, but they do not develop AIDS even in the absence of antiretroviral therapy (8-10). Taken together, these data suggest that Nef is a key factor in HIV pathogenesis to AIDS, and validate Nef as a strong target for future antiretroviral therapy.

1.2 HOST CELL INTERACTIONS WITH HIV-1 NEF

Nef has been shown to downregulate surface receptors in HIV-infected cells, including CD4 (11-13) and MHC-I (14-16). The Nef-induced endocytosis of CD4 occurs soon after HIV infection (17-19), and is mediated by AP-1 and clathrin-coated pits that direct CD4 to endosomal degradation via lysosomes (20). The downregulation of cell surface CD4 is beneficial to the virus because it prevents HIV superinfection (21) and enhances release of virion particles (22-24) from the cellular membrane. Recent evidence also implicates Nef-associated CD4 downregulation as integral to the evasion of the potent, anti-viral response known as antibody-dependent cell-mediated cytotoxicity (25, 26). Interaction of CD4 with HIV Env proteins on the cell surface is important for exposure of epitopes that are recognized by neutralizing Env antibodies. By downregulating CD4, HIV Nef prevents antibody recognition and thus promotes immune evasion of HIV-infected cells.

Another group of cell surface proteins that are downregulated by HIV Nef are encoded by the major histocompatibility complex 1 (MHC-I). MHC-I genes encode receptor proteins that present peptide antigens on the infected cell surface for recognition by cytotoxic T lymphocytes (CTLs) (27). It is beneficial for the virus to down regulate MHC-I to protect the infected cell from the CTL response to HIV antigens (15, 27). There are two mechanisms that have been described for MHC-I downregulation: rapid internalization of surface-exposed MHC-I (14, 16), and direct trafficking to clathrin-coated vesicles instead of the plasma membrane from the trans-Golgi (28). To complete the downregulation of MHC-I, Nef works by recruiting the clathrin adaptor protein AP-1 to the cytoplasmic tail of MHC-I (29), displaying a different downregulation mechanism than CD4 internalization, which involves the AP-2 clathrin adaptor.

Nef also targets T-cell receptor signaling pathways as well as anti-apoptotic pathways (27, 30, 31). These pathways are affected by Nef interaction with a variety of host cell kinases, which are normally part of signal generation and propagation pathways linked to T cell activation. By interacting with kinases, Nef adjusts kinase regulation and catalytic activity, resulting in either activation or inhibition of the specific kinase involved. Two families of kinases that interact directly with Nef are described in more detail in the following sections.

1.3 HIV-1 NEF AND SRC FAMILY KINASES

The Src family of non-receptor protein-tyrosine kinases (SFKs) is among the best understood kinase families that interact with Nef. Src family kinases adopt a domain organization that includes a myristoylated N-terminal arm, followed by Src homology 3 (SH3) and Src homology 2 (SH2) domains, the catalytic kinase domain, and a short C-terminal tail (**Fig. 1a**). The myristate group on the N-terminus of all SFKs promotes the association of these kinases with membranes, and is required for SFK cellular function.

Structural studies show that interdomain interactions between the SH3, SH2, and kinase domains regulate Src-family kinase activity (32-38). SH3 domains bind proline-rich regions that adopt left-handed polyproline type II (PPII) helices, while SH2 domains bind short peptide recognition motifs containing phosphotyrosine. In the absence of an activating signal, SFKs adopt an autoinhibited conformation in which the SH3 domain packs against the N-lobe of the kinase domain via an interaction with the SH2-kinase linker (**Fig. 2a**). This linker adopts a PPII helical fold for interaction with the SH3 binding pocket. This holds the SH2 domain against the C-lobe. A phosphorylated tyrosine on the C-terminal tail binds in the SH2 binding pocket, acting as a

clamp to hold the entire downregulated structure together (SFK structure reviewed in (39-41)). Phosphorylation of the C-terminal tail tyrosine is catalyzed by an independent regulatory kinase known as Csk (42).

Nef activates some SFK members – notably Hck, Lyn, and c-Src – by interacting with the SH3 domains of these kinases (35, 36). When Nef binds the SH3 domain via a conserved PXXP motif, the SH3 domain is displaced from the autoinhibited conformation, and the SFK is activated (37). Recent hydrogen deuterium exchange studies suggest that Nef-induced activation of Src-family kinases correlates with only a subtle change in the overall conformation of the active complex (43). Structures of Nef:SFK complexes will be described in more detail below.

The Nef-mediated activation of SFKs is a key piece of the functionality of Nef. Selective inhibitors of Nef-dependent SFK activation inhibit HIV-1 replication *in vitro* (44, 45), and in primary macrophages knockdown of Hck expression inhibits HIV-1 replication (46). The activation of SFKs has also been shown to contribute to the Nef-dependent down modulation of MHC-I (47) as described above.

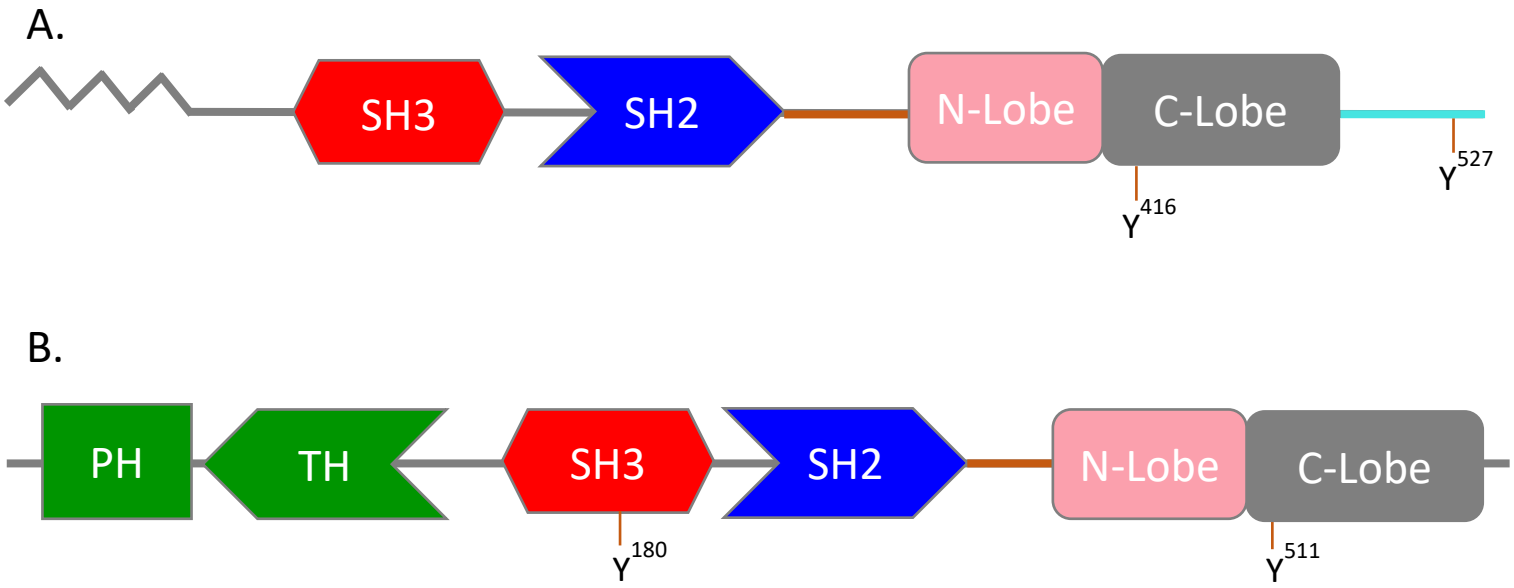

Figure 1. Domain organization of Src and Tec Famliy Kinases. A) Domain structure of SFKs. Src family kinases are comprised of a myristoylated N-terminal region, a SH3 domain, SH2 domain, SH2-kinase linker, tyrosine kinase domain, and a C-terminal tail. Tyr 416 is the site of activation loop phosphorylation, while Tyr 527 is phosphorylated by Csk in the autoinhibited state. B) Domain structure of TFKs. Tec family kinases are comprised of a PH domain, TH motif, SH3 domain, SH2 domain, SH2-kinase linker and tyrosine kinase domain. Tyr 511 is the site of activation loop phosphorylation, while autophosphorylation of Tyr 180 results in modified ligand binding.

1.4 HIV-1 NEF AND TEC FAMILY KINASES

Published work from our group has shown that Nef also interacts with several members of the Tec family of protein-tyrosine kinases (TFKs). Tec kinases are modular in domain organization, containing SH3, SH2, and tyrosine kinase domains in a Src-like arrangement. The Src-like module is preceded by a Pleckstrin homology (PH) and a Tec homology (TH) domain (**Fig. 1b**), which are also involved in kinase regulation. There is no N-terminal myristate group; instead, the PH domain supports membrane recognition and binding. The TH motif is N-terminal to a proline-rich region that is implicated in an intramolecular domain association with the SH3 domain (48), and which competes with the SH2-kinase linker for SH3 engagement.

1.4.1 Structural Biology of Bruton's Tyrosine Kinase (Btk)

The 2015 model of autoinhibited Btk (49), which is found in all hematopoietic cells except for T cells and NK cells, highlights the similarities and differences between SFKs and TFKs. Kuriyan *et al.* (2015) solved the X-ray crystal structure of a PH-TH-kinase protein and a SH3-SH2-kinase protein and used these structures to build a model of the full structure. The authors built a full length model by aligning the kinase domains of each individual X-ray structure and subjecting the alignment to molecular dynamics relaxation. The relaxed model (**Fig. 2b**) reveals a compact domain organization similar to the autoinhibited form of the Src-family kinase Hck, albeit with some key differences (49). The SH3 domain of Btk is packed against the N-lobe of the kinase domain and interacts with the SH2-kinase linker, analogous to the downregulated Hck structure.

Unlike Hck, however, Btk appears to utilize the PH-TH domain module as a clamp to hold the autoinhibited structure together instead of a phosphorylated C-terminal tail. The PH-TH module sits atop the kinase domain, and is packed against the back of the SH3 domain. This arrangement exposes the lipid-binding site of the PH domain for membrane interaction, and leaves the SH3 domain available for displacement by a high affinity ligand (49). While this model of autoinhibited Btk provides important new insight into TFK downregulation, the mechanism of TFK activation is still unclear. The model proposed has been validated through a variety of techniques in competing laboratories, and while the compact, autoinhibited Src-like core has been shown to be reproducible, the site of PH domain packing on the kinase domain has been called into question. HIV-1 Nef may provide a unique probe to address this important question, as it has in the past for Hck and other Src-family kinases.

A series of more recent publications from the Andreotti and Engen labs have proposed that Btk is regulated by more than just the SH2-kinase linker interaction with the SH3 domain. These further regulatory effectors include Trp395 in the kinase linker (50, 51), the proline-rich-region found upstream of the SH3 domain and PH domain interaction with lipid ligands (52). These groups have used a combination of nuclear magnetic resonance (NMR), hydrogen-deuterium exchange mass spectrometry (HDX-MS), and molecular dynamics simulations to probe these interactions and learn more about the regulation of Btk in solution. Trp395, which is located in the SH2-kinase linker and sits at the top of the N-lobe of the kinase domain, affects the activation state of the kinase based on which rotamer conformation is adopted (51). If this residue is mutated, the kinase is less active due to the disruption of the regulatory spine in the kinase domain, which negatively affects the allosteric movement of the kinase domain as a whole (50, 51). Similarly, the proline rich region (PRR) that is N-terminal to the SH3 domain also acts as an activator of kinase

signaling (52), in contrast to the SH2-kinase linker proline region, which is involved in autoinhibition (50). As shown in complementary HDX-MS and NMR experiments (52), this N-terminal PRR competes with the SH2-kinase linker to bind the SH3 domain and affect kinase activation. When the PRR is bound to the SH3 domain, the kinase is in an active conformation, but when the SH2-kinase linker is bound to the SH3 domain the kinase is inactive. This set of experiments, in combination with work from the Kuriyan lab, also highlights the role of lipid binding to the PH domain (49, 52, 53). When the PH domain is bound by a lipid ligand (e.g., PI(3,4,5)P3 or soluble IP6) the kinase adopts a more active conformation. This is achieved through a structural rearrangement of the entire Btk protein, that unwinds the compact autoinhibited structure (49) into an active linear array of domains previously described by small-angle X-ray scattering (54). It is important to realize that for Btk, activation is not an 'on/off switch' but instead acts more like a 'dimmer switch', regulating the amount of activation based on the combination of regulatory factors (52). These interactions, taken together, tightly regulate Btk kinase, but not all of these interactions are found in TEC family member Itk. Compared to Btk, Itk regulation is still poorly understood, due in part to the difficulty of producing soluble Itk proteins for use in structural and/or biochemical studies. This thesis seeks to develop methods by which a larger library of Itk and Btk proteins can be produced on a scale sizeable enough for use in structural biology.

1.4.2 HIV-1 and Interleukin-2-inducible T-cell kinase (Itk)

Of the five TFKs, Itk in particular has been shown to affect multiple stages of the HIV-1 life cycle including viral entry, transcription from the viral LTR, virion assembly and release (55). Itk is found in T cells, NK cells, and mast cells where it functions as part of the response to T cell

activation downstream of the T cell receptor (53, 56-59). Btk has also been implicated in the HIV life cycle, with Btk specific inhibitors showing promising results against HIV-1 infected cells (60). Using a cell-based bimolecular fluorescence complementation (BIFC) assay, our group established that Nef interacts directly with Itk, Btk, and Bmx through their SH3 domains at the plasma membrane (61). Nef was also shown to induce Itk activation in transfected cells, and a selective inhibitor of Itk catalytic activity was shown to block HIV infectivity and replication in a Nef-dependent manner (61), but only in cells where HIV-1 replication is enhanced by Nef. These studies are important because they provide the mechanistic bridge between HIV-1 and the host cell kinase Itk. They also suggest an SH3 domain displacement mechanism for Itk activation by Nef; which comprises part of my thesis project to address this possibility from a biochemical and structural perspective.

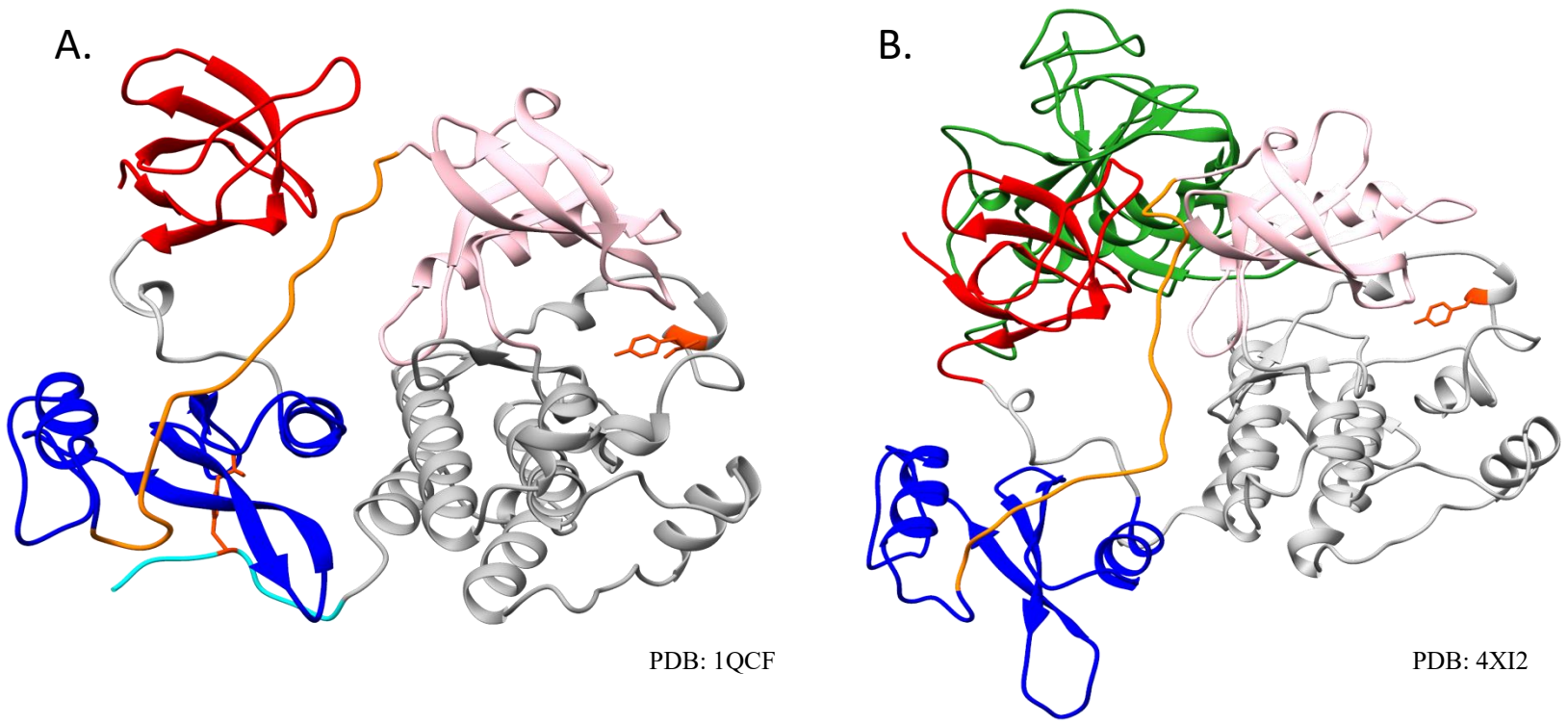

Figure 2. Comparison of down-regulated SFKs and TFKs. A) X-ray crystal structure of down-regulated, auto-inhibited Hck. The two interactions that define the auto-inhibited kinase are the engagement of the SH2-kinase linker (orange) by the SH3 domain (red), and the binding of pTyr 527 from the C-terminal tail (cyan) into the SH2 domain (blue) binding pocket. Together, these interactions hold Hck in a compact, inactive structure. Upon activation, loop Tyr 416 is phosphorylated. Subtle displacement of the SH3 domain from SH2-linker engagement is sufficient to activate the kinase. B) Model of auto-inhibited Btk. The Btk SH3-SH2-kinase core adopts a similar conformation as autoinhibited Hck. Unlike SFKs, Tec-family kinases lack a regulatory C-terminal tail. Instead, the PH-TH domain (green) clamps the kinase in the inactive state. This model of autoinhibited Btk was built utilizing two crystal structures relaxed together using molecular dynamics simulations.

1.5 STRUCTURES OF HIV-1 NEF IN COMPLEX WITH KEY HOST CELL EFFECTORS

HIV-1 Nef is a 27 kDa N-myristoylated protein containing a flexible N-terminal arm (residues 1-56), a proline-rich loop (57-80), a well-structured core domain (81-206, Δ148-180) and a C-terminal flexible loop (148-180) (62). The N-terminal arm of Nef is responsible for membrane localization, which requires the myristate group to be exposed, as well as a basic patch of residues further down the arm (62). There have been several X-ray crystal structures solved of Nef in complex with a variety of host proteins (32-34, 63, 64), a subset of which are described below. In all structures reported to date, the Nef core adopts a nearly identical three-dimensional fold despite its ability to interact with diverse host cell proteins.

1.5.1 Nef : AP-2 α-σ2 hemicomplex

The clathrin adaptor protein AP-2 is the mechanistic link by which Nef downregulates cell surface CD4, as described above. Ren *et al.* (2014) solved the structure of the Nef core, including the C-terminal loop, in complex with the AP-2 α-σ2 hemicomplex. The majority of contacts between Nef and the AP-2 hemicomplex are located in the Nef C-terminal loop, which adopts a fold containing two helices, an acidic-dileucine motif, and a series of turns. A helix that comprises residues 167-170 and a segment of turns (171-179) are packed between Nef and AP-2, allowing for the visualization of the entire C-terminal loop for the first time by X-ray crystallography. While the majority of interactions between AP-2 and Nef are located in the loop, the Nef core also packs

against the AP-2 hemicomplex. Previous mapping of Nef residues that interact with the cytoplasmic tail domain of CD4 (65) indicate that these residues are still available for interaction once Nef has bound AP-2, providing a model of Nef-dependent association between the CD4 tail and the clathrin adaptor AP-2. This study (64) also highlights a possible advantage of crystallizing proteins with flexible regions in complexes with binding partners. In the case of Nef, the complex with AP-2 provided the first structure of the Nef internal loop, which was unstructured in all previous Nef X-ray crystal structures.

1.5.2 Nef : MHC-I : AP-1 μ1

Another key function of Nef is the downmodulation of MHC-I from the cell surface to protect HIV-infected cells from CTL- induced cell death (15, 27). Nef mediates this response by acting as an adaptor between MHC-I in the *trans*-Golgi network and the μ1 subunit of AP-1. In order to visualize the ternary interaction between the cytoplasmic domain (CD) of MHC-I, the μ1 subunit of AP-1, and Nef, Jia *et al.* (2012) used a Nef-MHC-I CD fusion protein to bind μ1 AP-1 for crystallographic analysis. The fusion of Nef and MHC-I CD was in a flexible region of Nef, so the authors believe the structure is free from artifacts (63). The structure reveals that the complex of Nef with AP-1 μ1 engages the MHC-I CD in a binding groove that is only present when Nef and AP-1 come together. In the absence of Nef, the MHC-I binding motif for AP-1 (Yxxφ motif) does not engage the AP-1 μ1 binding pocket due to the lack of a large hydrophobic residue at Y+3 (φ= alanine in MHC-I). When Nef is present, however, a sidewall is formed at the pocket creating a more favorable groove for MHC-I binding (63). The sidewall is comprised of the Nef proline-rich

region, which then pre-organizes Nef for long range electrostatic interactions with μ1 AP-1 and MHC-I (63). These electrostatic interactions hold the ternary complex together, and involve Asp123 of Nef, which is highly conserved and critical to this and other Nef functions. This structure, in conjunction with the Nef:AP-2 structure highlights the diverse functionality of Nef. Nef interacts with both adaptor proteins, but through different mechanisms and binding sites, indicating that the mechanism of Nef partner protein binding is not always predictable based on previous structures.

1.5.3 Nef : Hck SH3-SH2

In addition to adaptor proteins, Nef also binds and activates members of Src kinase family as described above (32-38). Among these, the Hck SH3-SH2 dual domain has been solved in complex with Nef (32) (as has the Hck SH3 domain in earlier work (66)). The structure of the Nef:Hck SH3-SH2 complex revealed previously unknown contacts between the SH3 domain and Nef, as well as contacts between SH2 and Nef, and a novel Nef:Nef dimer interface. As described earlier, SH3 domains contain two binding grooves on their surface that recognize the Nef PXXP motif that adopts a polyproline type II helix. This expected interaction is observed in the complex, plus a new salt-bridge between residues Nef Arg105 and SH3 Glu93, which was shown to be critical for Nef:Hck complex formation and activation of the kinase (32). The structure also revealed a system of van der Waals contacts between the Hck SH2 domain and Nef, which was previously unknown. While a Nef-Nef dimer interface was visualized in previous Nef:SH3 (34, 66) structures as well as the Nef:Hck SH3-SH2 (32) structure, the dimer interface varies between them. While the Nef residues involved in the dimer interfaces overlap, there are some key differences that

expose residues important for other functions. Most interesting is the observation that engagement of Hck SH3-SH2 exposes Nef Asp123, which is critical to both CD4 and MHC-I downregulation. This observation suggests that interaction with Hck may reorganize the Nef dimer to allow interaction with endocytic adaptor proteins, and is consistent with the requirement for Hck in the MHC-I downregulation pathway. More generally, the differences in quaternary structure between Nef when bound to SH3 vs. SH3-SH2 speak to the importance of solving structures that contain as much of each partner protein as possible.

1.6 ADDITIONAL STRUCTURAL FEATURES OF HIV-1 NEF

1.6.1 Nef Dimerization

The Nef dimers that have been observed (**Fig 3.)** in X-ray crystal structures (32, 34, 66) are not merely artifacts of crystallization conditions. These dimers are dependent on the binding partner of the Nef protein, and are generally oriented around the αB helix. While the helix that forms the dimer interface is the same across the dimers, the orientation of that helix varies greatly between the structures. This indicates that Nef may be pre-organized for binding certain partners based on the dimerization state of the core molecule. Nef homodimers have been observed in cells through BiFC studies (67), and mutagenesis of the Nef dimerization interface based on these crystal structures have established that dimerization is required for various functions of Nef. These functions include CD4 and MHC-1 downregulation (67, 68), Src-family kinase activation (32), and HIV infectivity and replication (67). It is even possible to interfere with various functions of Nef though the use of small molecules that bind and disrupt Nef dimerization (69), indicating that

the quaternary structure of Nef is vital to its interactions with other molecules. This quaternary structure appears to be responsible, at least in part, for the ability of Nef to interact with a multitude of binding partners, and has now been observed in several different orientations.

1.6.2 Nef Myristoylation

In cells, Nef is N-terminally myristoylated in order to promote association with cellular membranes, where much of the function of Nef is carried out (70, 71). This myristoylation, covalently attached at Gly2, is necessary for many of the functions of Nef, and has been implicated in the binding of Nef to sites of activity (70, 71). Interestingly, many of the proteins that are known to interact with Nef functionality are also targeted to cellular membranes via an assortment of different pathways. These partners include Src and Tec-family kinases, as well as endocytic adaptor complexes and membrane receptors as described in the preceding sections. While the role of myristoylation in Nef function is well known, the atomic-level structure of full-length myristoylated Nef is undetermined. Models based on low resolution structural studies have been conducted, and will be discussed in further detail in following sections. Thus another important goal of this project was to develop methods for production of full-length, myristoylated Nef protein for biophysical studies in model lipid bilayers.

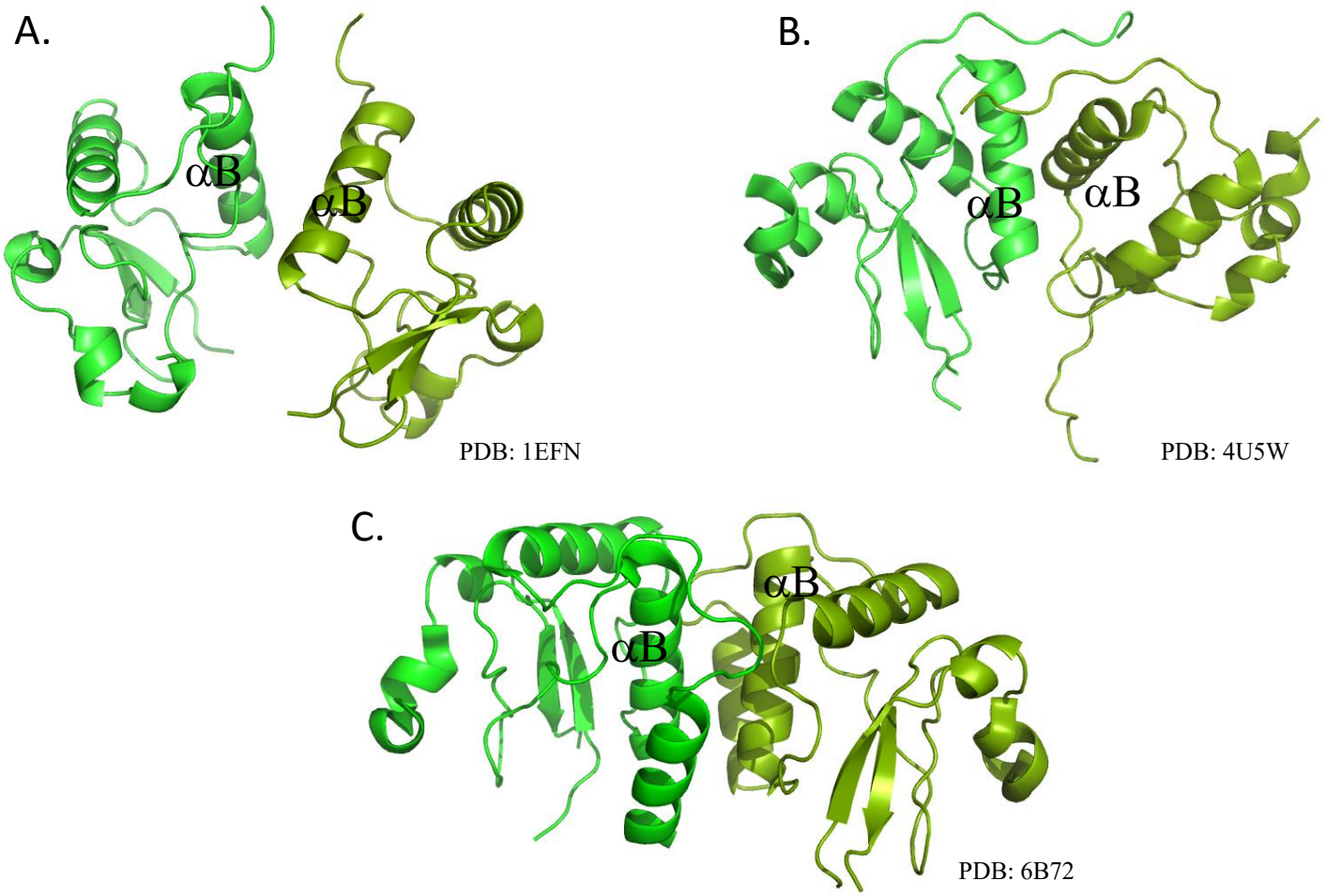

Figure 3. HIV-1 Nef Dimers in Selected Crystal Structures. A) Nef bound to Hck SH3 domain results in a dimer of complexes that orients the αB helix of Nef into the dimer interface. B) Nef bound to Hck SH3-SH2 results in a dimer that is reoriented around the same αB helix interface, but the orientation is different from that seen in A. C) Nef bound to a single β-octyl glycoside detergent molecule (not shown) dimerizes in yet another orientation that utilizes the αB helix in a novel fashion. This function of Nef, to dimerize around the αB helix in a ligand- or partner protein-dependent manner, may explain how Nef associates with diverse host cell proteins for the advantage of HIV-1. The Nef monomer is virtually unchanged in each structure.

2.0 MATERIALS AND METHODS

2.1 BACTERIAL EXPRESSION VECTORS

2.1.1 Itk His_6 Tagged Library

Multiple expression constructs were designed based on previous structural data, and were PCR-amplified and subcloned into the pET-30a(+) vector via Nco1 and Xho1 restriction sites to yield a library of plasmids for expression of C-terminally His_6-tagged Itk proteins. The final expression library consisted of Itk SH3, SH3-SH2, PH-SH3-SH2, and PH-SH3 proteins. The Itk SH3-SH2 P287A, and PH-SH3-SH2 R96P/T110I/P287A mutants were created with site-directed mutagenesis using the parent plasmids described above and the QuickChange II XL site-directed mutagenesis kit (Stratagene). The Itk R96P/T110I mutant was prepared by J. Reese, a former undergraduate student in our lab, who performed site-directed mutagenesis on the parent plasmid described as above.

2.1.2 Btk /Itk Smt3 Tagged Library

An expression library consisting of N-terminally Smt3-tagged Btk and Itk proteins was PCR-amplified (from plasmids gifted from A. Andreotti, Iowa State University) and subcloned into the pET-28a(+) vector containing N-terminally His6-tagged Smt3 (gift from P. Thibodeau, University of Pittsburgh) via Bam-HI and XhoI restriction sites. The final expression library consisted of Itk SH3, SH2 WT, SH2 P287A, PH-SH3-SH2 R96P/T110I/P287A, and Btk SH3, SH2, PH-SH3-SH2, PH-SH3, SH3-SH2. All proteins in this library contained the N-terminal Smt3-tag.

2.1.3 Nef SF2 Proteins

The full length and core Nef SF2 allele vectors were obtained from Dr. John Jeff Alvarado and encompassed residues 1-209 and 58-209, respectively in a pET-21a(+) backbone. The Nef PP76,79AA mutant was created by site-directed mutagenesis using the parent plasmids described and the QuickChange II XL site-directed mutagenesis kit (Stratagene).

2.1.4 Full Length Myristoylated Nef SF2

Myristoylated Nef was produced through the use of a pET-Duet 1 plasmid encoding full-length Nef SF2 with a C-terminal His_6 tag and human N-myristoyl transferase-1 (hNMT-1) (72), which was kindly provided by Dr. John Engen (Northeastern University, Boston MA). The Myr-Nef D123N mutant was produced with site-directed mutagenesis using the parent plasmid and the QuickChange II XL site-directed mutagenesis kit (Stratagene)

2.2 EXPRESSION AND PURIFICATION FROM BACTERIAL VECTORS

2.2.1 Itk His_6 Tagged Protein Library

All expression constructs were used to transform *Escherichia coli* (*E. coli*) strain Rosetta2(DE3) pLysS (EMD Millipore), and a single colony used to inoculate starter cultures of LB media. Starter cultures were grown overnight at 37°C, and then diluted 100-fold into 1 liter fresh LB. Expression cultures were grown at 37°C until OD_{600} of 0.8, and then cooled to 15°C for 1 hr. Cooled cultures were induced with 1 mM isopropyl 1-thio-β-D-galactopyranoside (IPTG), and left overnight for protein expression. After 16 h, cells were collected by 4,000g centrifugation, snap-frozen in liquid nitrogen, and stored at -80C.

Purification of the Itk His_6 protein library was carried out on 1 L cell pellets (~5g), which were thawed on ice and resuspended into Ni-IMAC binding buffer (25 mM Tris-HCl, pH 8.3, 0.5 M NaCl, 20 mM imidazole, 10% v/v glycerol, 2 mM β-mercaptoethanol [BME]). Pellets were fully homogenized with a protease inhibitor pellet (cOmplete, EDTA-free; Sigma) according to manufacturer recommendations, and passed through a microfluidizer (Microfluidics) 10-12 times at 4°C. The cell lysate was then spun at 56,000Xg for 1 hr at 4°C to clarify. The clarified lysate was loaded onto a pre-equilibrated 5 mL HIS-TrapHP column (GE Healthcare) at 2.0 mL/min. Bound protein was washed with 5-column volumes of binding buffer before being eluted over a 32-column volume linear gradient between 20 mM and 500 mM imidazole using Ni-IMAC elution buffer (binding buffer with 500 mM imidazole). Fractions containing the protein of interest were identified using SDS-PAGE gels, pooled, and dialyzed overnight into ion exchange binding buffer (25 mM Tris, pH 8.0, 1 mM EDTA, 10% v/v glycerol, 4 mM BME) using a 3-kDa cut-off

membrane (Millipore). Following dialysis, the protein was loaded onto a either pre-equilibrated 5 mL Q-TrapHP or SP-TrapHP column (GE Healthcare) at 2.0 mL/min, and washed with 5-column volumes binding buffer, before being eluted over a 32-column volume linear gradient between 0 0.5 M NaCl using ion exchange elution buffer (binding buffer with 1M NaCl). Fractions containing the protein of interest were pooled and concentrated on an Amicon stirred-cell concentrator with a 3-kDa membrane to a volume of approximately 10 mL. The protein was then buffer exchanged with size exclusion buffer (20 mM Tris-HCl, pH 8.3, 150 mM NaCl, 1 mM EDTA, 10% v/v glycerol, and 2 mM Tris (2-carboxyethyl) phosphine [TCEP]) and further concentrated to a final volume of less than 6 mL, followed by centrifugation at 10,000 rpm for 10 min at 4°C to pellet any insoluble precipitate. The soluble protein was loaded onto a pre-equilibrated HiLoad 16/60 Superdex 75 gel filtration column (GE Healthcare), and eluted at a flow rate of 0.5mL/min. Fractions containing the protein were assayed by SDS-PAGE, pooled, concentrated, flash-frozen in liquid nitrogen, and stored at -80°C for use.

2.2.2 Btk /Itk Smt3 Tagged Library

All Smt3-tagged proteins were expressed in the *E. coli* strain Rosetta2(DE3) pLysS (EMD Millipore) using the same procedure as described for His_6 tagged proteins above.

Purification of the Btk/Itk Smt3 library of proteins was carried out on 1 L cell pellets (~5g), which were thawed on ice and resuspended into Ni-IMAC binding buffer (25 mM Tris-HCl, pH 8.3, 0.5 M NaCl, 20 mM imidazole, 10% v/v glycerol, 2 mM TCEP). Pellets were fully homogenized with a protease inhibitor pellet (cOmplete, EDTA-free; Sigma) according to manufacturer recommendations, and passed through a microfluidizer (Microfluidics) 10-12 times

at 4°C. The cell lysate was then spun at 110,000Xg for 1 h at 4°C to clarify. The clarified lysate was loaded onto a pre-equilibrated 1 mL His GraviTrap column (GE Healthcare) and allowed to drip through under atmospheric pressure at 4°C. The bound protein was then washed with 30-column volumes of binding buffer, before being eluted with 3 mL elution buffer (binding buffer supplemented with 500 mM imidazole). If the Smt3 tag was to be removed, the 3mL elution was diluted into 50 mL binding buffer and rocked overnight at 4 °C in the presence of SUMO-protease at a ratio of 10,000:1 protein:protease. Following cleavage, the sample was run over the same His GraviTrap column, and the flow-through collected. This flow-through was then concentrated to 6 mL, and buffer exchanged into size-exclusion buffer (same as above). If cleavage was not desired, the 3 mL elution was diluted 2-fold in size exclusion buffer and then dialyzed overnight into the size exclusion buffer over a 3-kDa membrane (Millipore). The full 6 mL sample (either cleaved or uncleaved) was then loaded onto a pre-equilibrated HiLoad 16/60 Superdex 75 gel filtration column (GE Healthcare), and eluted at a flow rate of 0.5 mL/min. Fractions containing the protein were pooled, concentrated, flash-frozen in liquid nitrogen, and stored at -80°C for use.

2.2.3 Nef SF2 Proteins

All Nef proteins were expressed in the *E. coli* strain Rosetta2(DE3) pLysS (EMD Millipore) using the same procedure as described for His_6 tagged proteins above, with the modification of 25 °C induction temperature instead of 15 °C.

Purification of the full length and core Nef proteins was carried out on 2 L cell pellets (~10 g), which were thawed on ice and resuspended into anion exchange binding buffer (25 mM Tris-HCl, pH 8.0, 1 mM EDTA, 10% v/v glycerol, 4mM BME). Pellets were fully homogenized with

a protease inhibitor pellet (cOmplete, EDTA-free; Sigma) according to manufacturer recommendations, and passed through a microfluidizer (Microfluidics) 10-12 times at 4°C. The cell lysate was then spun at 110,000Xg for 1 h at 4 °C to clarify. The clarified lysate was loaded onto a pre-equilibrated 5mL Q-TrapHP column (GE Healthcare) at 2.0 mL/min. Bound protein was washed with 5-column volumes of binding buffer before being eluted over a 32-column volume linear gradient between 20 mM and 500 mM NaCl using ion exchange elution buffer (binding buffer with 1M NaCl). Fractions containing the protein of interest were pooled, and diluted into cation exchange binding buffer (25 mM HEPES, pH 7.5, 1 mM EDTA, 10% v/v glycerol, 1 mM DTT) The protein was loaded onto a pre-equilibrated 5 mL SP-TrapHP column (GE Healthcare) at 2.0 mL/min, and washed with 5-column volumes binding buffer, before being eluted over a 32-column volume linear gradient between 0 to 0.5M NaCl using cation exchange elution buffer (binding buffer with 1M NaCl). Fractions containing the protein of interest were pooled and concentrated on a Amicon stirred-cell concentrator with a 10-kDa membrane to a volume of approximately 10 mL. The protein was then buffer exchanged with size exclusion buffer (20 mM Tris-HCl, pH 8.3, 150 mM NaCl, 1 mM EDTA, 10% v/v glycerol, 2 mM TCEP) and further concentrated to a final volume of less than 6 mL, followed by centrifugation at 17,000 g for 10 min at 4 °C to pellet any insoluble precipitate. The soluble protein was loaded onto a pre-equilibrated HiLoad 16/60 Superdex 75 gel filtration column (GE Healthcare), and eluted at a flow rate of 0.5 mL/min. Fractions containing the protein were pooled, concentrated, flash-frozen in liquid nitrogen, and stored at -80°C for use.

2.2.4 Full length Myristoylated Nef SF2

The pET-Duet 1 plasmid containing Nef SF2 and hNMT-1 into *E. coli* strain Rosetta2(DE3) pLysS (EMD Millipore) using the protocol provided by the Engen lab (71). Briefly, a single colony used to inoculate starter cultures of freshly mixed M9 medium consisting of 1 mM $CaCl_2$, M9 salts and trace elements, 100 mM HEPES, pH 7.4, 1% casamino acids, 2% glucose, and 2 mM $MgSO_4$. Starter cultures were grown overnight at 37°C, and then diluted 100-fold into 1 L of fresh M9 minimal medium. Expression cultures were grown at 37 °C until OD_{600} of 0.6, at which time the medium was supplemented with myristic acid (Sigma) solution to 50 μM. Myristic acid solution was previously prepared as a 5 mM stock solution in 0.6 mM BSA, heated to 60 °C and pH corrected to 9.0 with NaOH, in order to promote solubilization. Following the addition of myristic acid, the cultures were shaken at 37°C for 1 hr, then cooled to 15 °C for 1 h. Cooled cultures were induced with 1 mM IPTG and left overnight. After 16 h, cells were collected into 1 L pellets by centrifugation, snap-frozen in liquid nitrogen, and stored at -80C.

Purification of myristoylated Nef proteins was carried out on 2 L cell pellets (~5 g), which were thawed on ice and resuspended into Ni-IMAC lysis buffer (20 mM Tris-HCl, pH 8.3, 100 mM NaCl, 20 mM imidazole, 10% v/v glycerol, 2 mM TCEP, 1% Triton X-100). Pellets were fully homogenized with a protease inhibitor pellet (cOmplete, EDTA-free; Sigma) according to manufacturer recommendations, and passed through a microfluidizer (Microfluidics) 5-7 times at 4°C. The cell lysate was then spun at 110,000Xg for 1 hr at 4°C to clarify. The clarified lysate was loaded onto a pre-equilibrated 5 mL HIS-TrapHP column (GE Healthcare) at 2.0 mL/min. Bound protein was washed with 30-column volumes of lysis buffer before being washed with 30-column volumes of Ni-IMAC wash buffer (lysis buffer with 25 mM sodium cholate instead of Triton X-

100). Then, the bound protein was washed with Ni-IMAC wash buffer (lysis buffer without Triton X-100), and finally eluted over a 32-column volume linear gradient between 20 mM and 500 mM imidazole using Ni-IMAC elution buffer (wash buffer with 500 mM imidazole). Fractions containing Myr-Nef (but not hNMT-1) were pooled and concentrated on a Amicon stirred-cell concentrator with a 10-kDa membrane to a volume of approximately 10 mL. The protein was then buffer exchanged with size exclusion buffer (20 mM Tris-HCl, pH 8.3, 150 mM NaCl, 10% v/v glycerol, 2 mM TCEP) and further concentrated to a final volume of approximately 10 mL, followed by centrifugation at 10,000 rpm for 10 min at 4 °C to pellet any insoluble precipitate. The soluble protein was loaded onto a pre-equilibrated HiLoad 16/60 Superdex 75 gel filtration column (GE Healthcare), and eluted at a flow rate of 0.5 mL/min. Fractions containing the protein were pooled, concentrated, and stored at 4 °C for use. One aliquot was sent to Jamie Morocco (Engen Lab, Northeastern University, Boston MA) for characterization of the ratio of myristoylated vs. non-myristoylated protein in the final sample.

2.3 SURFACE PLASMON RESONANCE (SPR)

SPR analysis was performed on a BIAcore T100 instrument (GE Healthcare) using a CM5 carboxymethyl dextran chip. The full-length Nef SF2 ΔC210 protein was covalently attached to the four-channel chip via standard amine coupling chemistry in HBS-EPD buffer (10 mM HEPES, pH 7.5, 150 mM NaCl, 3 mM EDTA, 0.05% v/v P20 surfactant, 1 mM DTT). All Itk and Btk proteins were then flowed past the immobilized Nef protein channel and a reference channel in HBS-EPD buffer at a flow rate of 10 μL/min for 2 min, followed by a 2 min dissociation period and surface regeneration step of increased flow of HBS-EPD buffer at 40 μL/min for 5 min. The

results were corrected for buffer effects and fitted to 1:1 binding model using the BIAcore T100 evaluation software.

3.0 RESULTS AND ANALYSIS

3.1 PROTEIN PURIFICATION

The purification of multiple proteins for the use in biochemical and biophysical assays comprised a significant portion of time in the laboratory during my thesis research and will be addressed in detail in the following sections. The Nef proteins that I utilized throughout the research were primarily purified from plasmids kindly provided by Dr. John Jeff Alvarado. I purified these proteins based on standard laboratory protocols, as outlined above, and they were generally concentrated to greater than 1 mg/mL with a yield greater than 10 mg per liter, with variations based on batches. In the following experiments, full-length Nef SF2 ΔC210 was utilized as a ligand in SPR experiments to the Itk proteins produced. Other Nef proteins that I produced in my time in the lab include Nef core SF2 ΔC210 (59-209) and the full-length Nef SF2 ΔC210 - PP76, 79AA mutant which lacks the proline residues essential for SH3 binding. While these proteins will not be described in the following results, they are available in the lab for use in future experiments.

3.1.1 Itk His_6 Library

The first plasmids produced and tested for expression and purification in this collection of proteins were the wild type Itk SH3, Itk SH3-SH2, and the Itk PH-SH3-SH2 constructs. Of these, the Itk SH3 and Itk SH3-SH2 proteins were readily expressed, and soluble at higher than 3 mg/mL concentrations in gel filtration buffer. Unfortunately, the Itk PH, Itk PH-SH3, and Itk PH-SH3-SH2 wild type proteins were not expressed as soluble proteins in *E. coli*, and required multiple mutations to promote soluble protein expression based on literature precedent for Btk. The first mutations were directed to the α-helix of the PH domain (73). This pair of mutations (R96P/T110I) comprise the flanking residues of the PH domain α-helix and are mutated to match the analogous residues in the Btk PH domain. Unfortunately, while the expression of the Itk PH protein was improved by the inclusion of the mutations, the amount of soluble protein after the 3-step purification process was negligible. However, the longer construct of Itk PH-SH3-SH2 was improved by the inclusion of the two PH domain mutations. The Itk PH-SH3 protein was not affected by the PH domain mutations, and could not be expressed in soluble form under any tested condition. In contrast to the PH domain containing proteins, Itk SH3-SH2 was highly soluble and produced protein on the order of greater than 20 mg per liter of induced bacterial culture. However, this protein displayed two peaks on elution from the Superdex 75 gel filtration column, with one peak elution volume consistent with monomer protein and one with dimer protein. These peaks were separated for use in subsequent experiments. To promote conversion of the Itk SH3-SH2 protein to the monomeric form, Pro287 was mutated to Ala (74), which was successful in reducing the amount of dimeric Itk SH3-SH2 protein found in the final SEC elution profile (**Figure 4**). The Pro287Ala substitution was also introduced into the Itk PH-SH3-SH2 construct. While the Itk PH-

SH3-SH2 triple mutant is still not a highly soluble protein, the cumulative addition of these three mutations was able to promote soluble protein expression to about 3 mg per liter. A summary of all the proteins produced for the Itk protein domain library are shown in **Table 1** and **Figure 8 i**n **Appendix B**.

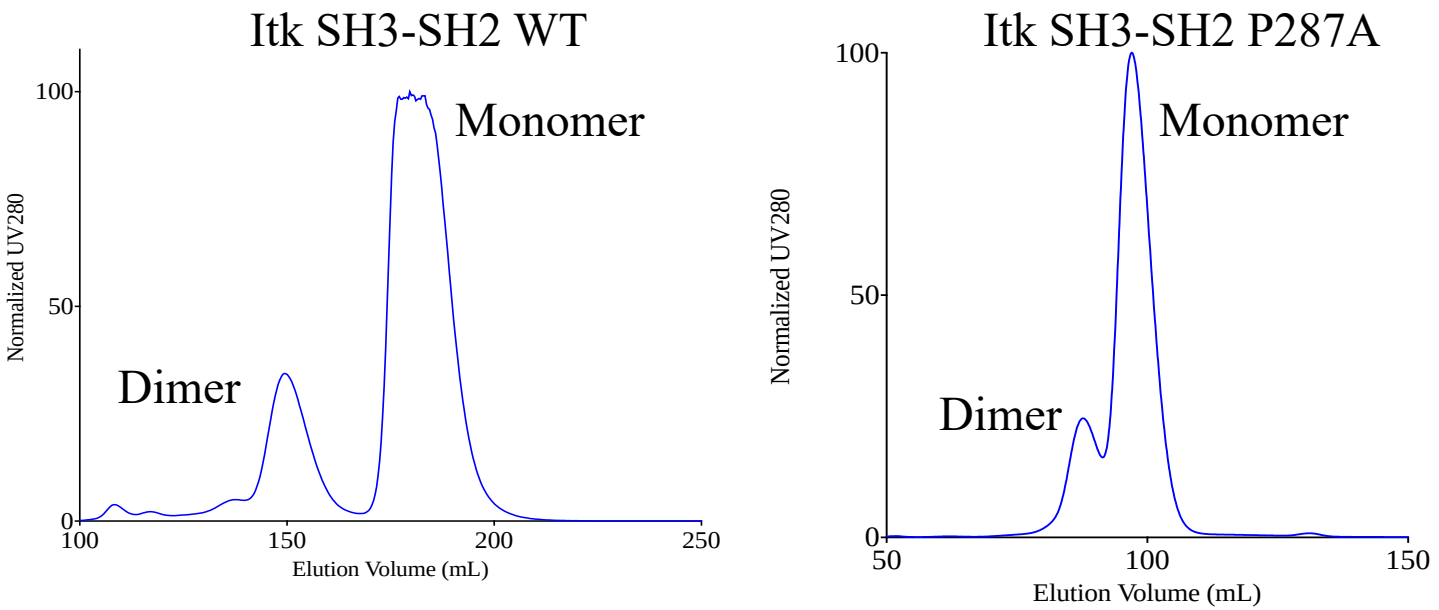

Figure 4. Size Exclusion Chromatography of Itk SH3-SH2 WT and P287A. Itk SH3-SH2 elutes from a gel filtration column as two species, one corresponding to a dimer and one corresponding to a monomer. Making a mutation in the SH2 domain to prevent a cis isomerization of P287 reduces the ratio of dimer produced in the final product, and has no negative impact on the solubility of the final protein.

3.1.2 Btk/Itk Smt3 Library

Following the limited success of expression of soluble C-terminal His_6-tagged Itk proteins, another method was needed to produce a significant amount of proteins that contained the PH domain. At the same time, it was decided to pursue Btk proteins concurrently with Itk proteins in the hope that Btk may provide an easier path to sufficient quantities of longer PH domain-containing proteins. To that end, a pET28a(+) plasmid that contained a N-terminal Smt3 tag was obtained from Dr. Patrick Thibodeau and an assortment of Btk and Itk proteins were pursued. The Itk SH3 and SH3-SH2 proteins were not remade in this new backbone since they were successful expressed in the earlier library. A full component of Btk domain proteins were produced, along with a set of complementary Itk proteins that were not successful in the His_6 tag vector. These proteins are summarized in **Table 2** and **Figures 9** and **10** in **Appendix B**. While the goal was to use the Smt3 tag to solubilize the proteins before cleaving the tag and leaving an untagged protein for use in experiments, this proved to be incompatible with some of the Btk and Itk proteins produced. Again, the PH domain-containing proteins proved to be problematic. All of the Btk and Itk proteins that contained a PH domain must be left with the Smt3 tag uncleaved in order to produce enough soluble protein for biophysical experiments. Proteins that do not contain a PH domain do not require the tag to be soluble, and proved to be expressed at a high level and amenable to cleavage, with yields of over 5 mg from 1 liter of culture. The yield of cleaved PH domain containing proteins was less than 0.5 mg from 1 liter of culture, but the yield was improved to over 1 mg per liter when the tag was left uncleaved.

Table 1. Summary of Itk Proteins Expressed with C-terminal His_6 Tags.

Protein	Domain(s)	Mutation(s)	MW (Da)	pI	ε ($M^{-1}cm^{-1}$)	State [a]	Yield (mg/L)
Itk	SH3	WT	8679.4	5.14	18450	Monomer	>20
Itk	SH3-SH2	WT	21542.0	6.16	37360	Monomer	>20
Itk	SH3-SH2	WT	43084.0	6.16	37360	Dimer	6
Itk	SH3-SH2	P287A	21516.0	6.16	37360	Monomer	>20
Itk	PH	R96P/T110I	21085.2	9.66	32430	----------	----------
Itk	PH-SH3	R96P/T110I	28550.3	8.78	50880	----------	----------
Itk	PH-SH3-SH2	WT	41412.9	8.97	69790	----------	----------
Itk	PH-SH3-SH2	R96P/T110I	41365.9	8.89	69790	Monomer [b]	1
Itk	PH-SH3-SH2	R96P/T110I/P287A	41339.9	8.89	69670	Monomer [b]	3

[a]State refers to the predicted oligomerization state of protein eluted off the Superdex75 gel filtration column and based on observed elution volume compared to known standards

[b]These proteins were observed to precipitate/oligomerize in solution during concentration

Table 2. Summary of Btk and Itk Proteins Expressed with N-terminal Smt3 Tags.

Protein	Domain(s)	Mutation(s)	MW with Smt3 (Da)	pI	MW without Smt3 (Da)	Smt3 Tag[a]	Yield (mg/L)
Btk	PH-TH	WT	34523.4	9.25	20739.9	Uncleaved	>20
Btk	PH-TH-SH3	WT	45730.0	8.77	31946.6	Uncleaved	>20
Btk	PH-TH-SH3-SH2	WT	57482.3	8.92	43698.9	Uncleaved	>20
Btk	SH3-SH2	WT	32881.9	6.21	19098.5	Cleaved	6
Btk	SH2	WT	25019.2	9.44	11235.8	Cleaved	3
Btk	SH3	WT	21129.6	4.45	7346.2	Cleaved	7
Itk	PH-TH	R96P/T110I	33756.5	9.66	19973.1	Uncleaved	3
Itk	SH2	WT	27006.4	9.08	13222.9	Cleaved	10
Itk	SH2	P287A	26980.4	9.08	13196.9	Cleaved	>20
Itk	PH-TH-SH3-SH2	R96P/T110I/P287A	54058.2	8.97	40274.8	Uncleaved	1

[a]Refers to the recommended state of Smt3 tag cleavage for soluble, concentrated final protein

3.2 SPR OF ITK SH3 AND ITK SH3-SH2

In a pilot experiment to determine if Itk was capable of binding Nef, full-length Nef SF2 was covalently bound to a CM5 chip on a BIAcore T100 instrument (GE Healthcare), and the soluble Itk SH3 and Itk SH3-SH2 proteins were flowed over to determine the kinetics and affinity of binding. The Src-family kinase Hck has been used extensively in the lab as a positive control for Nef binding, and was used in these experiments to show that the bound Nef was functional. As seen in **Figure 5**, Itk SH3 did not show binding to the full-length Nef unlike the Hck SH3 domain. This result suggests that the Itk SH3 domain alone is not sufficient for interaction with Nef, unlike the Hck SH3 domain. In contrast to the isolated Itk SH3 domain, the dual SH3-SH2 Itk protein readily bound to Nef. The Itk SH3-SH2 monomeric protein bound full-length Nef with a similar affinity as the Hck SH3-SH2 protein (3.35×10^{-7} M vs. 2.34×10^{-7} M, respectively), but with much different binding kinetics (**Table 3**). The Itk SH3-SH2 had a much slower rate of dissociation than Hck SH3-SH2 from Nef, and required a regeneration step to fully remove the protein from Nef on the chip. As observed, the 1:1 binding model did not describe the Itk SH3-SH2 data well, so this data was also fit with a heterogeneous ligand model. This model accounts for two ligand molecules, or binding sites, to bind an analyte independently of each other. The Itk SH3-SH2 dimer protein also bound full-length Nef, but the extent of binding was greatly reduced (i.e., the response was much lower) indicating that the protein was not as robust a binding partner for Nef as the monomeric protein. These findings suggest that the mode of Nef interaction differs between Src and Tec family kinases, with the SH2 domain potentially having a bigger role in the Nef complex with Itk.

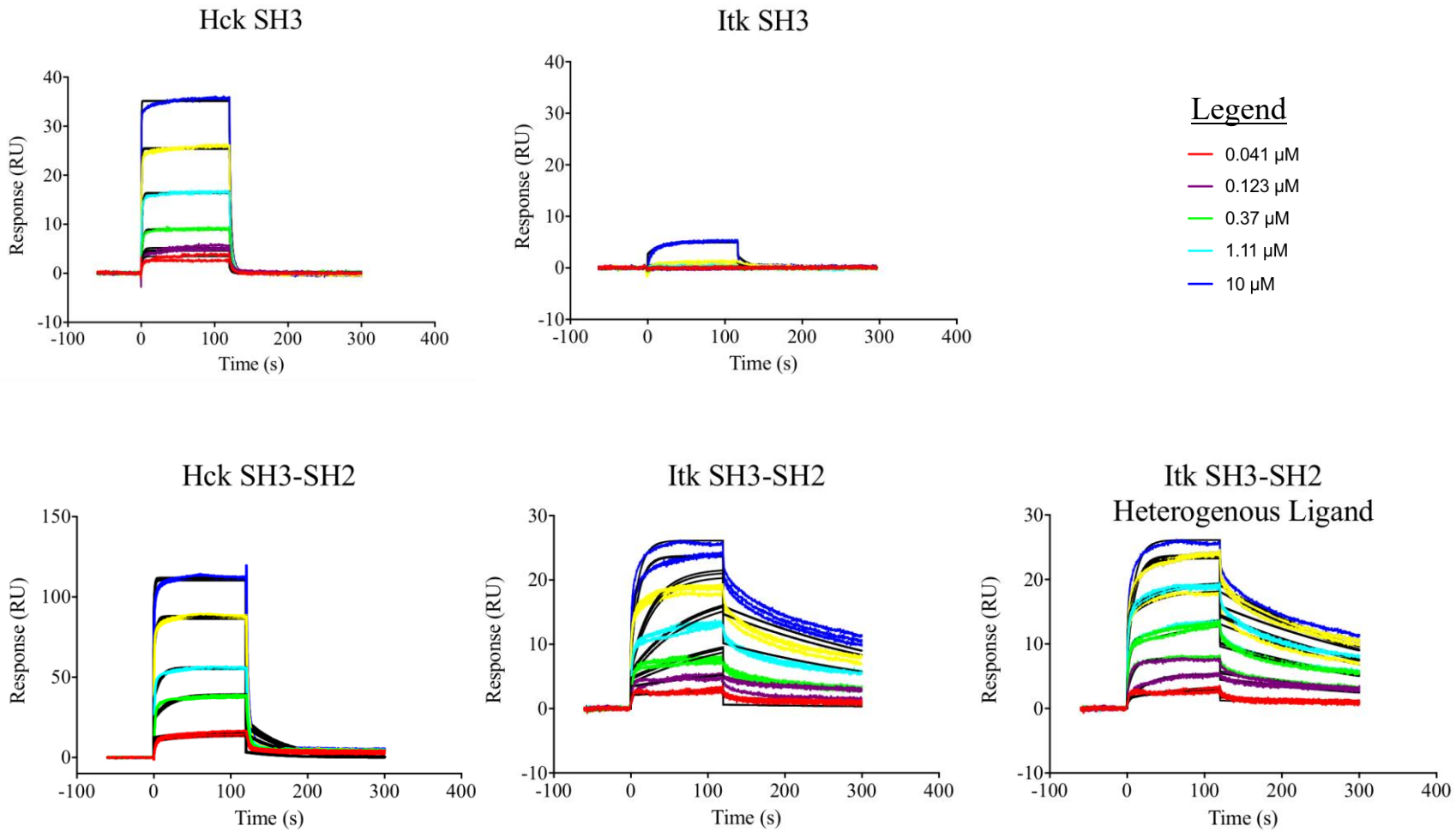

Figure 5. SPR of Itk SH3 and Itk SH3-SH2 to surface-bound full-length Nef SF2. Hck SH3 binds to FL Nef SF2 in a concentration dependent manner at K_D = 1.015x01^{-6} M, while Itk SH3 does not bind to FL Nef SF2, indicating a difference in how Nef interacts with these different tyrosine kinase families. Hck SH3-SH2 binds to FL Nef SF2 at a K_D = 2.34x10^{-7} and Itk SH3-SH2 binds Nef at a K_D = 3.35x10^{-7}, indicating that more than the Itk SH3 domain is necessary for Nef:Itk complex formation. All curves are fit with a 1:1 binding model to determine the K_D, unless otherwise noted. The fitted curves are shown as the black traces, while the experimental data are shown in color.

Table 3. Summary of SPR data.

Protein	k_{on} (M^{-1} sec^{-1})	k_{off} (sec^{-1})	K_D (M)	Chi^2
Hck SH3	2.79×10^{5}	0.38	1.015×10^{-6}	0.137
Itk SH3	N/A	N/A	No Binding	N/A
Hck SH3-SH2	8.93×10^{4}	2.09×10^{-2}	2.34×10^{-7}	15.6
Itk SH3-SH2	9.47×10^{3}	3.17×10^{-3}	3.35×10^{-7}	1.53
Itk SH3-SH2	1.14×10^{5}	6.55×10^{-3}	5.75×10^{-8}	0.602
Heterogeneous Ligand[a]	2775	1.30×10^{-3}	4.70×10^{-7}	

[a]This fitting model results in two values for each kinetic parameter, with a separate binding affinity for each set.

3.3 FULL-LENGTH MYRISTOYLATED NEF

The purification of full-length myristoylated Nef was undertaken for use in lipid SPR and neutron reflectometry studies in collaboration with Rebecca Eells and Mathias Lösche (Department of Physics, Carnegie Mellon University). The general protocol and plasmids were provided by Chris Morgan and John Engen (Northeastern University). Following the published protocol, each batch of the myristoylated Nef that I produced was checked by mass spectrometry for purity in the Engen lab before use. Generally, a single batch was purified from a 2-liter cell pellet, and yielded between 0.5 mg and 1 mg of protein at a concentration usually around 10 μM or less. Due to the instability of the myristic acid moiety on the N-terminus, this protein was not stored at -80°C, and was prepared fresh for each round of experiments. Each batch had a different ratio of myristoylated : non-myristoylated Nef, which was taken into consideration for each experiment. Two examples of a typical mass check result can be found in **Figure 6,** located in **Appendix A**. Before the protein was assayed in lipid SPR or other experiments, the stability of the protein was checked using a thermal melt assay. Full-length myristoylated Nef was stable for 24 h at room temperature in all salt buffer conditions tested (**Figure 7**). All experiments conducted on lipid membranes were conducted in 50mM NaCl in order to promote Myr-Nef binding to the membrane.

In collaboration with the Lösche group, association of recombinant purified Myr-Nef was tested for associated with artificial lipid bilayers using an SPR approach. For these studies, lipids are tethered to a gold surface, and association of the myristoylated and non-myristoylated forms of Nef was assessed as increases in the SPR signal. We found that the Myr-Nef protein associated readily with the lipid bilayer, with preliminary K_D values in the low micromolar range. Interestingly, once Myr-Nef associated with the membrane, it remained stably bound,

enabling further characterization by neutron reflectometry. In contrast, the non-Myr-Nef protein interacted weakly with the membrane and only at high concentrations. Together, these observations suggest that the use of the sparsely-tethered lipid bilayers and Myr-Nef will be a viable system for future structural studies of Nef:Itk and other effector complexes in the membrane environment.

4.0 DISCUSSION

4.1 ITK HIS_6 LIBRARY

The inclusion of the two α-helix mutations in the PH domain is necessary for the increased solubility of any Itk protein that contains the PH domain. It is also important to remember the inclusion of the PH domain in the Itk protein greatly affects the pI of the protein. The increased basicity of the proteins with PH domains must be taken into consideration when designing the purification conditions and future experiments. While the Itk PH and the Itk PH-SH3 proteins were not soluble even with the mutations included, the yield of Itk PH-SH3-SH2 was improved upon the inclusion of mutations.

Working towards the formation of a homogenous, soluble protein mixture that would be suitable for use in X-ray crystallography experiments, Pro287 in the SH2 domain was mutated t

Ala (74, 75). This mutation forces the residue at position 287 to adopt a *trans* conformation, which may be necessary to produce consistently monomeric Itk SH3-SH2 protein. The proline that is native to this position in Itk can adopt a *cis* or *trans* conformation and has been shown, by molecular dynamics simulations, to cause the Itk SH3-SH2 protein to oligomerize when in the *cis* conformation (74, 76). While oligomers larger than dimers were never observed in the soluble fraction eluted from gel filtration, it was necessary to spin the concentrated protein prior to gel filtration to remove a fine precipitate that would fall out of solution during concentration. This SH2 domain mutation was also added to the Itk PH-SH3-SH2 R96P/T110I protein to try to alleviate precipitation and oligomerization of the larger protein, and further promoted the expression of soluble Itk PH-SH3-SH2 protein.

The Itk PH-SH3-SH2 protein was purified multiple times, and there are several additives that can affect the solubility that were tested. The addition of the surfactant β-octyl glucoside was able increase the solubility of the final protein when included in the concentration buffer (before and after gel filtration). However, these proteins were being used in multiple assays by myself and others in the laboratory in experiments where the addition of this surfactant could be detrimental to the outcome of the assay. This is especially true in the case of testing the proteins in the lipid SPR setup in collaboration with the Lösche lab (Carnegie Mellon University). For this reason, the protein that was most commonly utilized did not contain detergent in the final buffer. If it was desirable to boost the final concentration of this protein (i.e., for use in X-ray crystallography) the addition of β-octyl glucoside may be a good starting point.

The addition of the soluble phosphoinositide PH domain ligand IP6 was also tested as a technique to boost solubility, but unfortunately it was not sufficient to increase the final yield or concentration of the protein. Previous studies have shown that IP6 is a potent activator of Btk

kinase activity (49). I also explored the interaction of IP6 with the Itk PH-SH3-SH2 protein in SPR experiments, which yielded a K_D value of approximately 0.3 mM (data not shown).

4.2 BTK/ITK SMT3 LIBRARY

The use of the Smt3 tag as a solubilization aid has been previously noted (77), and it proved to be equally successful for the production of both Btk and Itk proteins that were unsuccessful with a His_6 tag. However, it was not possible to take full advantage of the system as several of the proteins had to be left with the Smt3 tag, as they fell out of solution upon cleavage of the tag; including Btk PH, PH-SH3, PH-SH3-SH2, Itk PH R96P/T110I, and Itk PH-SH3-SH2 R96P/T110I/P287.

It is important to note that all ten of the proteins in this library had to be treated carefully during the dialysis from Ni-IMAC elution buffer into gel filtration buffer. All ten proteins experienced heavy precipitation at this step the first time they were purified. Subsequent attempts to prevent precipitation were most successful when the eluted protein was diluted by at least two times in the dialysis buffer, before being dialyzed overnight at 4°C. This gentle dialysis step seemed to help reduce precipitation. There was also heavy precipitation following cleavage of the Btk SH2 domain. It is recommended to dilute this protein before cleavage as well. This proved to be an easy, reliable way to minimize protein loss due to precipitation, and is recommended before any cleavage step as a precaution. Most of the precipitation noted during the purification of these proteins appeared to be related to protein concentration, so as long as the protein remained dilute (e.g. 1.0 mg/ml or less), the precipitation was minimal.

The protocol developed for these proteins utilized gravity fed columns that proved to be straightforward to use, and provided a way to purify a large number of proteins quickly and efficiently. However, because these columns only have a 1 mL bed volume it is important to restrict expression to a less rich media, like the standard LB media. While expression in a richer media like Terrific Broth (TB) can produce larger cell pellets (and subsequently more recombinant protein), TB pellets proved to be too large for these columns. Even though the cell lysates treated with benzonase and clarified by ultracentrifugation, the gravity-flow columns still became clogged. That said, it is likely that all of these proteins could be purified using standard 5 mL columns under the regulated flow of our automated purification systems. Nevertheless, the single-use Ni-IMAC gravity flow columns proved to be exceptionally amenable to the cleavage step, where the flow-through is collected (Smt3 tag contains an N-terminal His sequence for clean removal). Moving forward, I would recommend these columns for use with Smt3 tagged proteins, particularly those that will be cleaved before gel filtration chromatography.

4.3 FULL-LENGTH MYRISTOYLATED NEF

The experiments carried out by Rebecca Eells (Lösche laboratory, CMU) on the Myr-Nef I produced can be found in her Ph.D. thesis. Briefly, she determined that myristoylated Nef binds charged sparsely-tethered lipid bilayer membranes with a K_D of approximately 1 μM. The binding was robust enough for data to be collected during neutron reflectometry (NR) experiments, which revealed the core of Nef is suspended about 80 angstroms from the lipid membrane, while the myristate group inserts into the outer layer of the bilayer. Taken together, the lipid SPR and NR

experiments provide a good base for future experiments utilizing these techniques and proteins. It is necessary to take into account that each batch of Myr-Nef results in a limited amount of protein, so experiments regarding this protein have to be well planned in advance so that the protein can be utilized to its full extent. I tried to use protein within two or three weeks of purification. This is because the protein was stored at 4°C, as opposed to -80°C in small aliquots. NR experiments require 2.5 mL of protein at a concentration at least twice that of the K_D determined from SPR experiments, so it takes almost a full batch to complete a set of NR experiments.

5.0 FUTURE DIRECTIONS

In this thesis, I have presented the work put towards producing Itk and Btk proteins that can be utilized in a variety of biochemical and biophysical techniques to address the question of how Itk and Btk are activated both in the presence and absence of HIV-1 Nef. These proteins can be used to study the interaction between TFKs and Nef. I did not address the work put into producing full-length Btk and Itk and their use in biochemical assays. This work has already been picked up by others in the lab, and is promising for future success.

The first study I would advise would be a comprehensive analysis of which (if any) of the TFK proteins will form a stable complex with Nef in solution, the first step towards a crystallization trial. While I tried to form a complex between several of the Itk His_6 tagged proteins and Nef, I was not successful in forming a stable complex in solution. I mixed the proteins in a 1:1.2 ratio for an hour on ice and ran them over a Superdex 75 analytical column (GE Healthcare) to determine if a complex was formed. While this technique has shown success with Hck SH3-SH2 and Nef, ultimately leading to an X-ray structure (32), the Itk SH3-SH2 cHis_6 protein was not able to consistently form a complex with either the Nef core or full-length Nef proteins. I also attempted to co-express and co-purify these proteins together, but was unsuccessful in forming a

stable complex. It is entirely possible that Btk proteins would be more amenable to complex formation with Nef, or even one of the longer Itk constructs that are tagged with Smt3.

Complementary to the analytical gel filtration experiment, a comprehensive study of protein: protein interactions via SPR would be another experiment I would propose to be conducted. The results of this study may provide valuable preliminary data in advance of crystallization screens. Itk and Btk proteins that form high affinity interactions with Nef, or displayed a prolonged dissociation in a kinetic experiment, would be the ideal candidates to combine in crystallization trials going forward.

I set up four trays of crystallization trials pursuing a complex between Nef and the Itk SH3-SH2cHis$_6$., by simply mixing the proteins in a 1:1 ratio. Unfortunately, the attempt was unsuccessful and no crystals were observed either for the complex or the individual Itk protein. However, there are still many promising proteins and protein complexes that are available to test in co-crystallization studies. The Btk proteins in particular may be favorable as the Btk Src-like core has been crystallized (49) previously (see Introduction). While my proteins do not contain the kinase domain, they do contain the Smt3 tag, which might work to promote crystallization in the same way. Ideally, the crystals would be obtained from untagged protein, but those proteins that contain PH domains benefit greatly from the addition of the Smt3 tag in solubility and yield. However, any data collected with the Smt3 tag will need to be verified on untagged protein to ensure the tag is not inducing an artifact. Crystal trials should also be completed on the individual Itk proteins. There are currently no published X-ray structures of more than a single domain of Itk. The only Itk structure that contains two domains is an NMR structure of an individual SH3 domain bound to an isolated SH2 domain. For this reason, any structure that can be obtained from any of the larger constructs of Itk would be a major advance in the field of Itk structural biology.

The structure of Itk or Btk in complex with Nef will reveal the binding interface between two proteins that have been shown to be a mechanistic link between HIV infection and the T-cell signaling pathway (in the case of Itk). With a better understanding of how Nef activates and interacts with Itk it may be possible to design or discover small molecules that target the interaction and provide additional protection from the pathogenicity of HIV-1. The structure of the Itk:Nef complex may also reveal how Itk is activated for the first time, thus providing insight into not only HIV-1 biology, but also Itk activation.

APPENDIX A

ANALYSIS OF MYRISTOYLATED NEF PROTEINS

Before the full-length myristoylated Nef could be used in lipid SPR or nuclear reflectometry experiments it was necessary to get the mass check of each batch of protein (**Figure 6**). Each batch exhibited a different level of myristoylation, and this ratio of myristoylated to non-myristoylated protein was used to estimate the actual concentration of myristoylated Nef in each sample. The protein was also assayed for thermal stability at room temperature over a 24h period (**Figure 7**). This was to test if the protein would aggregate during a typical neutron reflectometry experiment.

January 2017

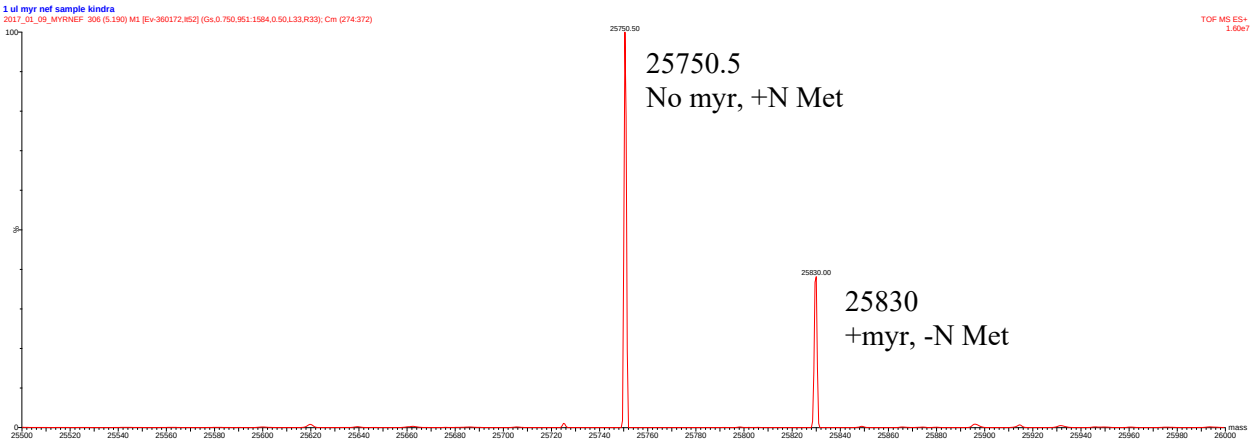

March 2017

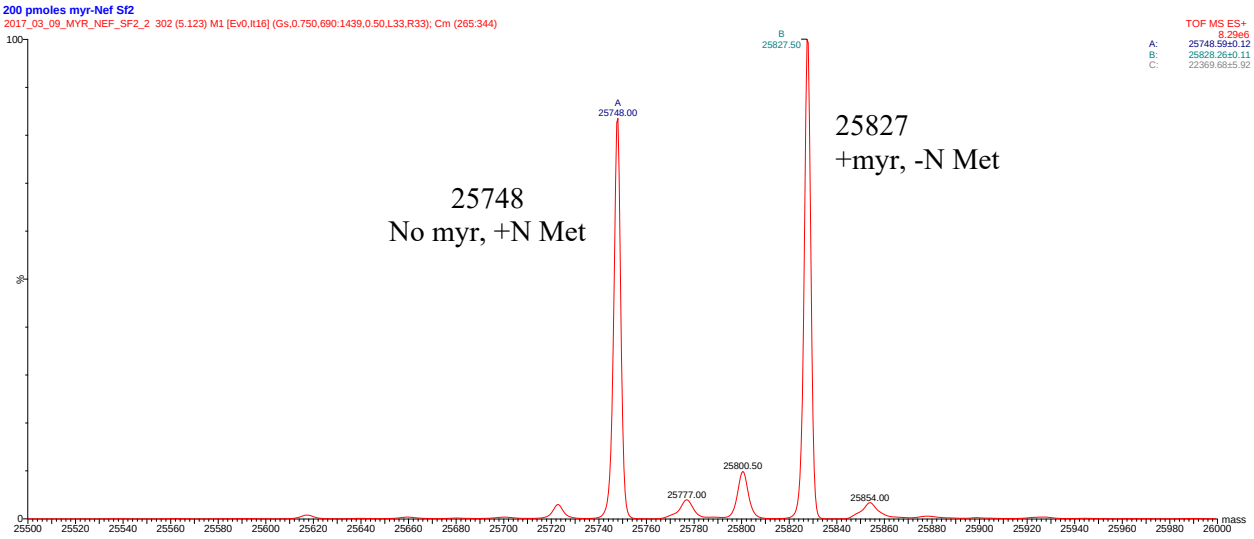

Figure 6. Mass Check of Selected Batches of Myr-Nef. Every time a new batch of myristoylated Nef had to be expressed and purified an aliquot from that batch was sent to the Engen Lab at Northeastern University for mass check. The best batch, WT Myr-Nef from March 2017 was approximately a 1:1 ratio of Myr : Non-Myr Nef. Most other batches were around 30% myristoylated, similar to the January 2017 batch shown. Some batches were 0% myristoylated and could not be used for lipid SPR studies.

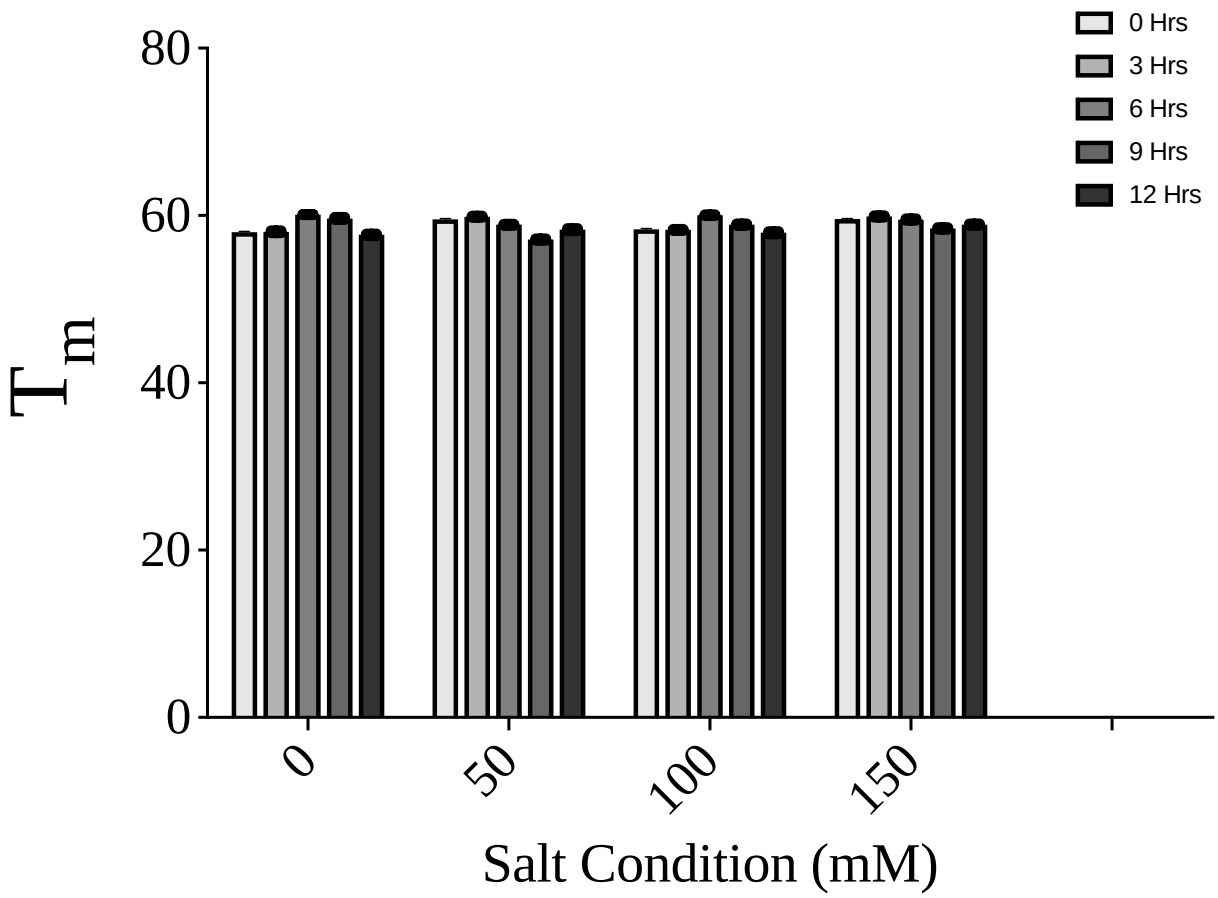

Figure 7. Thermal stability of Myr-Nef. The stability of full-length myristoylated Nef was determined to be stable over a 12 hour period in buffers containing 0-150 mM NaCl. This experiment was utilized to prove that the protein would not destabilize over the course of a typical neutron reflectometry experiment, even at low salt concentrations. Experiments were carried out at 50mM NaCl on lipid membranes.

APPENDIX B

SELECTED SDS-PAGE GELS OF PURIFIED PROTEINS

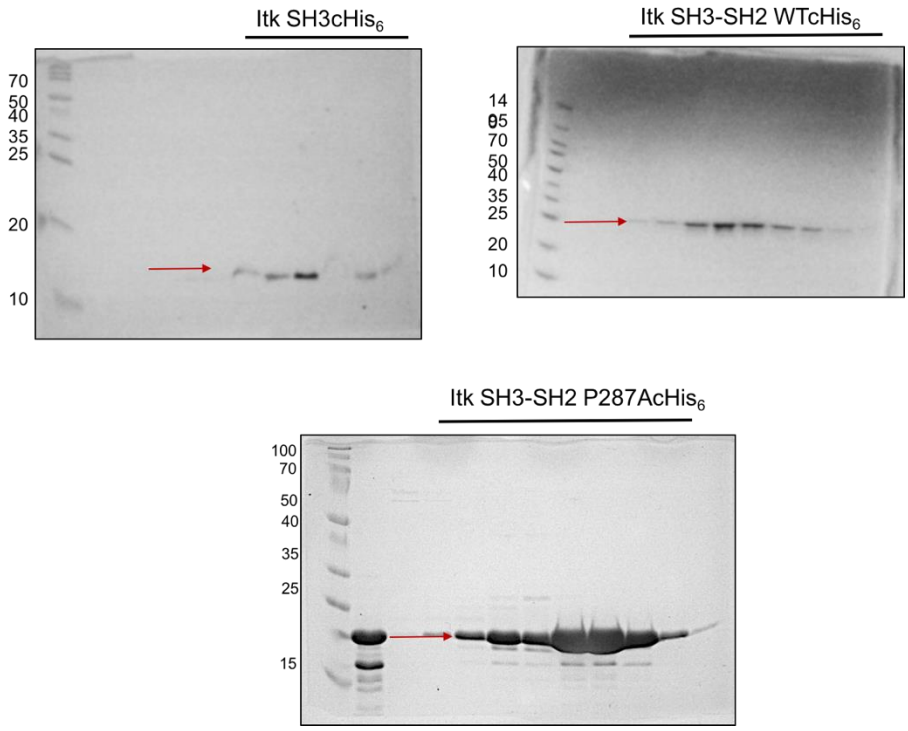

Figure 8. SDS-PAGE of Successful ItkcHis$_6$ Proteins. Protein was purified from a one liter expression as described in Methods. Gels shown are of the final protein fractions after gel filtration, but before concentration.

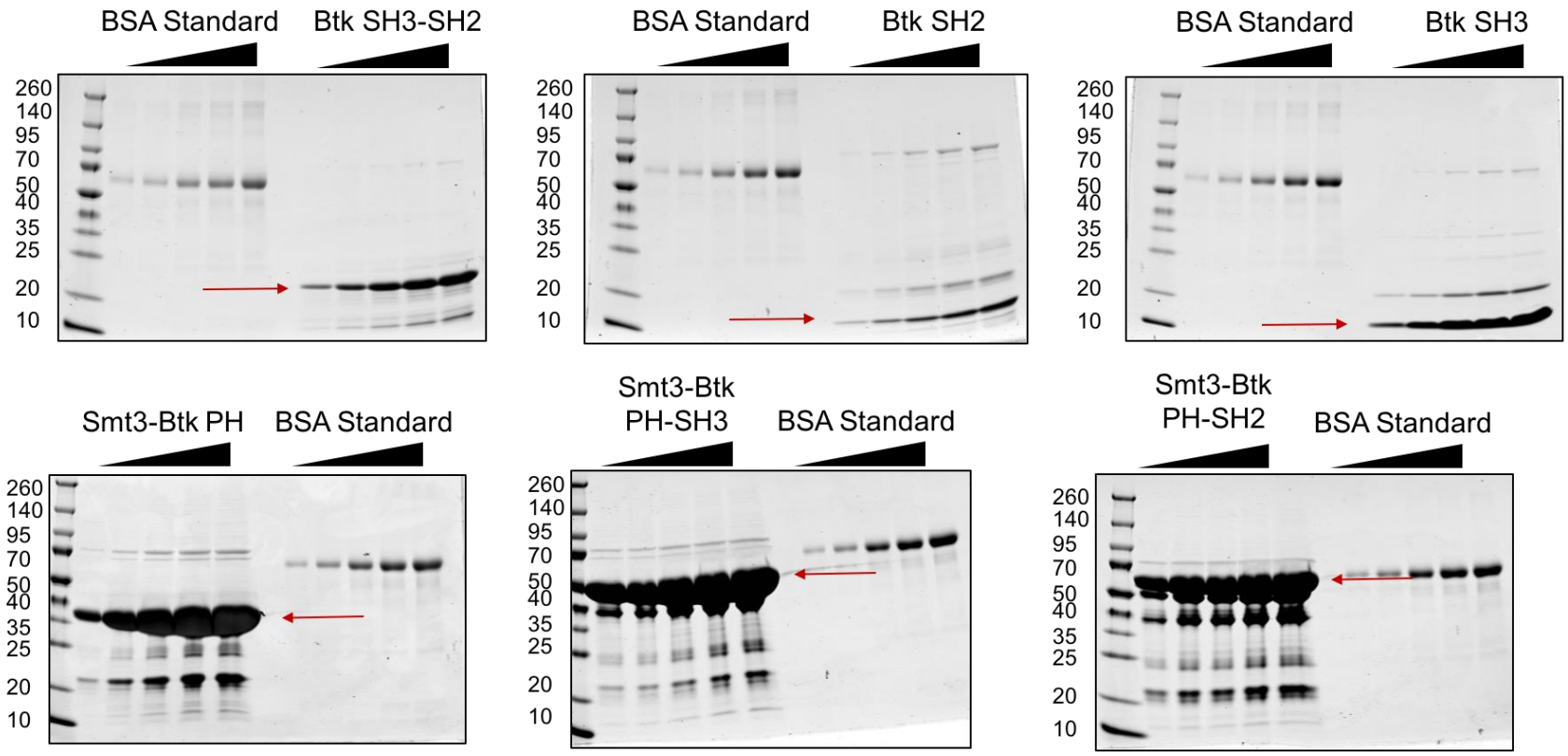

Figure 9. SDS-PAGE of Successful Btk-Smt3 Fusion Proteins. Protein was purified from a one liter expression as described in Methods. Gels shown are of the final protein assayed against a BSA standard of 0.5µg, 1µg, 2µg, 3µg, and 4µg. The name of the protein denotes if cleavage was utilized for the final protein. The BSA standard was used to calculate the final yield of protein in the 3mL sample.

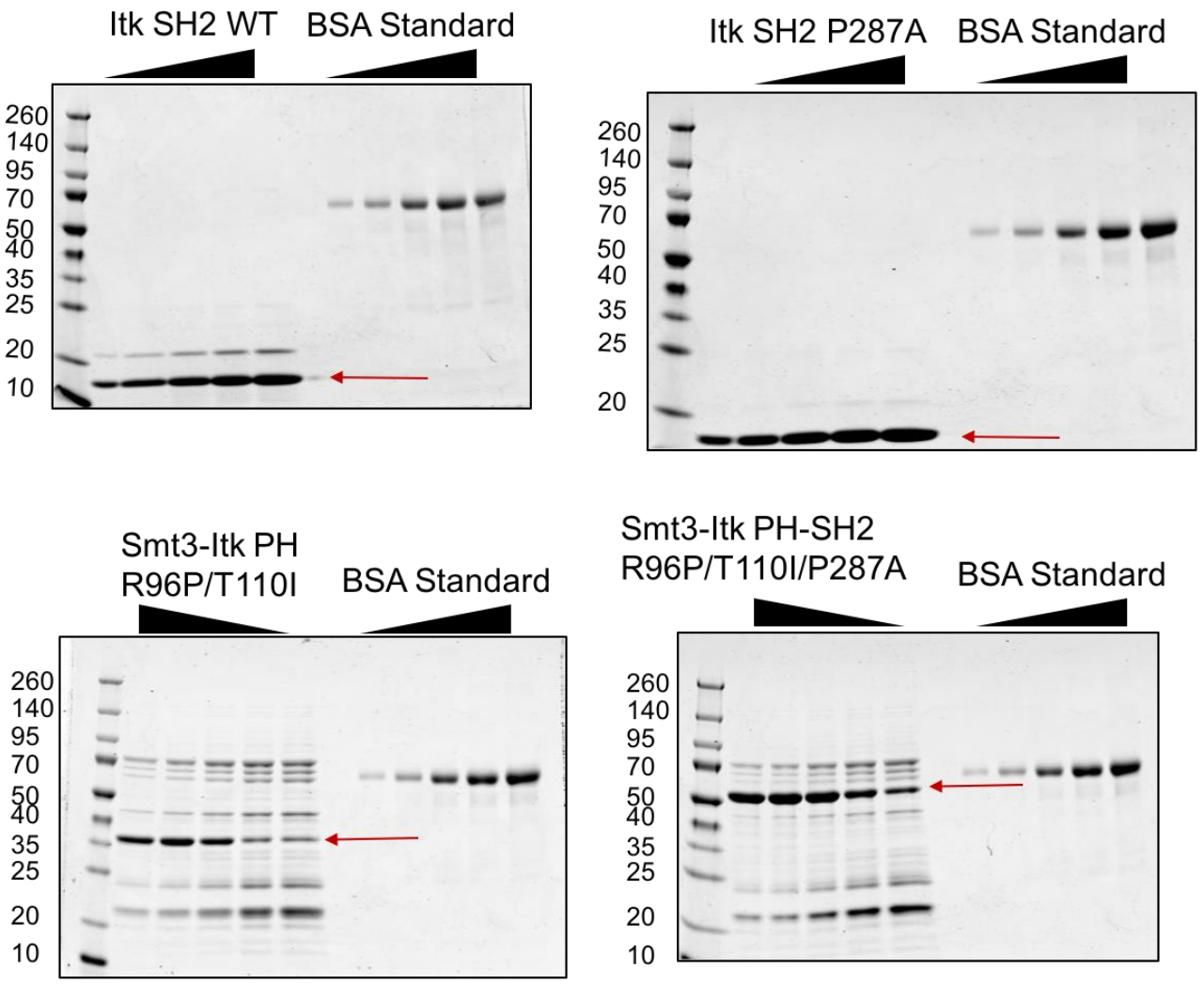

Figure 10. SDS-PAGE of Successful Btk-Smt3 Fusion Proteins. Protein was purified from a one liter expression as described in Methods. Gels shown are of the final protein assayed against a BSA standard of 0.5µg, 1µg, 2µg, 3µg, and 4µg. The name of the protein denotes if cleavage was utilized for the final protein. The BSA standard was used to calculate the final yield of protein in the 3mL sample.

BIBLIOGRAPHY

1. Stevenson M (2003) HIV-1 pathogenesis. *Nat Med* 9(7):853-860.
2. Esté JA & Cihlar T (2010) Current status and challenges of antiretroviral research and therapy. *Antiviral Research* 85(1):25-33.
3. Michaud V, *et al.* (2012) The Dual Role of Pharmacogenetics in HIV Treatment: Mutations and Polymorphisms Regulating Antiretroviral Drug Resistance and Disposition. *Pharmacological Reviews* 64(3):803-833.
4. Kwong PD, Mascola JR, & Nabel GJ (2012) The changing face of HIV vaccine research. *Journal of the International AIDS Society* 15(2):17407.
5. Adamson CS & Freed EO (2010) Novel approaches to inhibiting HIV-1 replication. *Antiviral Research* 85(1):119-141.
6. Kestier Iii HW, *et al.* (1991) Importance of the nef gene for maintenance of high virus loads and for development of AIDS. *Cell* 65(4):651-662.
7. Priceputu E, *et al.* (2005) The Nef-Mediated AIDS-Like Disease of CD4C/Human Immunodeficiency Virus Transgenic Mice Is Associated with Increased Fas/FasL Expression on T Cells and T-Cell Death but Is Not Prevented in Fas-, FasL-, Tumor Necrosis Factor Receptor 1-, or Interleukin-1β-Converting Enzyme-Deficient or Bcl2-Expressing Transgenic Mice. *Journal of Virology* 79(10):6377-6391.
8. Carl S, *et al.* (2000) Partial "Repair" of Defective NEF Genes in a Long-Term Nonprogressor with Human Immunodeficiency Virus Type 1 Infection. *Journal of Infectious Diseases* 181(1):132-140.

9. Kirchhoff F, Greenough TC, Brettler DB, Sullivan JL, & Desrosiers RC (1995) Absence of Intact nef Sequences in a Long-Term Survivor with Nonprogressive HIV-1 Infection. *New England Journal of Medicine* 332(4):228-232.

10. Salvi R, *et al.* (1998) Grossly Defective nef Gene Sequences in a Human Immunodeficiency Virus Type 1-Seropositive Long-Term Nonprogressor. *Journal of Virology* 72(5):3646-3657.

11. Anderson S, Shugars DC, Swanstrom R, & Garcia JV (1993) Nef from primary isolates of human immunodeficiency virus type 1 suppresses surface CD4 expression in human and mouse T cells. *Journal of Virology* 67(8):4923-4931.

12. Garcia JV & Miller AD (1991) Serine phosphorylation-independent downregulation of cell-surface CD4 by nef. *Nature* 350(6318):508-511.

13. Mariani R & Skowronski J (1993) CD4 down-regulation by nef alleles isolated from human immunodeficiency virus type 1-infected individuals. *Proceedings of the National Academy of Sciences of the United States of America* 90(12):5549-5553.

14. Hung C-H, *et al.* (2007) HIV-1 Nef Assembles a Src Family Kinase-ZAP-70/Syk-PI3K Cascade to Downregulate Cell-Surface MHC-I. *Cell Host & Microbe* 1(2):121-133.

15. Collins KL, Chen BK, Kalams SA, Walker BD, & Baltimore D (1998) HIV-1 Nef protein protects infected primary cells against killing by cytotoxic T lymphocytes. *Nature* 391(6665):397-401.

16. Blagoveshchenskaya AD, Thomas L, Feliciangeli SF, Hung C-H, & Thomas G (HIV-1 Nef Downregulates MHC-I by a PACS-1- and PI3K-Regulated ARF6 Endocytic Pathway. *Cell* 111(6):853-866.

17. Chen BK, Gandhi RT, & Baltimore D (1996) CD4 down-modulation during infection of human T cells with human immunodeficiency virus type 1 involves independent activities of vpu, env, and nef. *Journal of Virology* 70(9):6044-6053.

18. Crise B & Rose JK (1992) Human immunodeficiency virus type 1 glycoprotein precursor retains a CD4-p56lck complex in the endoplasmic reticulum. *Journal of Virology* 66(4):2296-2301.

19. Willey RL, Maldarelli F, Martin MA, & Strebel K (1992) Human immunodeficiency virus type 1 Vpu protein regulates the formation of intracellular gp160-CD4 complexes. *Journal of Virology* 66(1):226-234.

20. Aiken C, Konner J, Landau NR, Lenburg ME, & Trono D (1994) Nef induces CD4 endocytosis: Requirement for a critical dileucine motif in the membrane-proximal CD4 cytoplasmic domain. *Cell* 76(5):853-864.

21. Benson RE, Sanfridson A, Ottinger JS, Doyle C, & Cullen BR (1993) Downregulation of cell-surface CD4 expression by simian immunodeficiency virus Nef prevents viral super infection. *The Journal of Experimental Medicine* 177(6):1561-1566.

22. Argañaraz ER, Schindler M, Kirchhoff F, Cortes MJ, & Lama J (2003) Enhanced CD4 Down-modulation by Late Stage HIV-1 nef Alleles Is Associated with Increased Env Incorporation and Viral Replication. *Journal of Biological Chemistry* 278(36):33912-33919.

23. Lama J, Mangasarian A, & Trono D (1999) Cell-surface expression of CD4 reduces HIV-1 infectivity by blocking Env incorporation in a Nef- and Vpu-inhibitable manner. *Current Biology* 9(12):622-631.

24. Ross TM, Oran AE, & Cullen BR (1999) Inhibition of HIV-1 progeny virion release by cell-surface CD4 is relieved by expression of the viral Nef protein. *Current Biology* 9(12):613-621.

25. Richard J, *et al.* (2015) CD4 mimetics sensitize HIV-1-infected cells to ADCC. *Proceedings of the National Academy of Sciences* 112(20):E2687-E2694.

26. Pham T, Lukhele S, Hajjar F, Routy J-P, & Cohen E (2014) HIV Nef and Vpu protect HIV-infected CD4+ T cells from antibody-mediated cell lysis through down-modulation of CD4 and BST2. *Retrovirology* 11(1):15.

27. Piguet V & Trono D (2001) Living in oblivion: HIV immune evasion. *Seminars in Immunology* 13(1):51-57.

28. Kasper MR & Collins KL (2003) Nef-Mediated Disruption of HLA-A2 Transport to the Cell Surface in T Cells. *Journal of Virology* 77(5):3041-3049.

29. Roeth JF, Williams M, Kasper MR, Filzen TM, & Collins KL (2004) HIV-1 Nef disrupts MHC-I trafficking by recruiting AP-1 to the MHC-I cytoplasmic tail. *The Journal of Cell Biology* 167(5):903-913.

30. Foster JL & Garcia JV (2007) Role of Nef in HIV-1 Replication and Pathogenesis. *Advances in Pharmacology*, (Academic Press), Vol Volume 55, pp 389-409.

31. Greenway A, *et al.* (2003) HIV-1 Nef control of cell signalling molecules: Multiple strategies to promote virus replication. *Journal of Biosciences* 28(3):323-335.

32. Alvarado JJ, Tarafdar S, Yeh JI, & Smithgall TE (2014) Interaction with the Src Homology (SH3-SH2) Region of the Src-family Kinase Hck Structures the HIV-1 Nef Dimer for Kinase Activation and Effector Recruitment. *Journal of Biological Chemistry* 289(41):28539-28553.

33. Arold S, *et al.* (1997) The crystal structure of HIV-1 Nef protein bound to the Fyn kinase SH3 domain suggests a role for this complex in altered T cell receptor signaling. *Structure* 5(10):1361-1372.

34. Lee C-H, Saksela K, Mirza UA, Chait BT, & Kuriyan J (Crystal Structure of the Conserved Core of HIV-1 Nef Complexed with a Src Family SH3 Domain. *Cell* 85(6):931-942.

35. Lee CH (1995) A single amino acid in the SH3 domain of Hck determines its high affinity and specificity in binding to HIV-1 Nef protein. *EMBO J* 14:5006-5015.

36. Moarefi I, *et al.* (1997) Activation of the Sire-family tyrosine kinase Hck by SH3 domain displacement. *Nature* 385(6617):650-653.

37. Saksela K, Cheng G, & Baltimore D (1995) Proline-rich (PXXP) sequences in HIV-1 Nef bind to SH3 domains of a subset of Src kinases and are required for the enhanced growth of Nef+ viruses but not for down-regulation of CD4. *EMBO J.* 14:484-491.

38. Trible RP, Emert-Sedlak L, & Smithgall TE (2006) HIV-1 Nef Selectively Activates Src Family Kinases Hck, Lyn, and c-Src through Direct SH3 Domain Interaction. *Journal of Biological Chemistry* 281(37):27029-27038.

39. Boggon TJ & Eck MJ (0000) Structure and regulation of Src family kinases. *Oncogene* 23(48):7918-7927.

40. Roskoski Jr R (2004) Src protein–tyrosine kinase structure and regulation. *Biochemical and Biophysical Research Communications* 324(4):1155-1164.

41. Sicheri F & Kuriyan J (1997) Structures of Src-family tyrosine kinases. *Current Opinion in Structural Biology* 7(6):777-785.

42. Okada M (2012) Regulation of the Src Family Kinases by Csk. *International Journal of Biological Sciences* 8(10):1385-1397.

43. Wales TE, *et al.* (2015) Subtle Dynamic Changes Accompany Hck Activation by HIV-1 Nef and are Reversed by an Antiretroviral Kinase Inhibitor. *Biochemistry* 54(41):6382-6391.

44. Emert-Sedlak L, *et al.* (2009) Chemical Library Screens Targeting an HIV-1 Accessory Factor/Host Cell Kinase Complex Identify Novel Antiretroviral Compounds. *ACS Chemical Biology* 4(11):939-947.

45. Narute PS & Smithgall TE (2012) Nef Alleles from All Major HIV-1 Clades Activate Src-Family Kinases and Enhance HIV-1 Replication in an Inhibitor-Sensitive Manner. *PLoS ONE* 7(2):e32561.

46. Komuro I, Yokota Y, Yasuda S, Iwamoto A, & Kagawa KS (2003) CSF-induced and HIV-1–mediated Distinct Regulation of Hck and C/EBPβ Represent a Heterogeneous Susceptibility of Monocyte-derived Macrophages to M-tropic HIV-1 Infection. *The Journal of Experimental Medicine* 198(3):443-453.

47. Dikeakos JD, *et al.* (2010) Small Molecule Inhibition of HIV-1–Induced MHC-I Down-Regulation Identifies a Temporally Regulated Switch in Nef Action. *Molecular Biology of the Cell* 21(19):3279-3292.

48. Andreotti AH, Bunnell SC, Feng S, Berg LJ, & Schreiber SL (1997) Regulatory intramolecular association in a tyrosine kinase of the Tec family. *Nature* 385(6611):93-97.

49. Wang Q, *et al.* (2015) Autoinhibition of Bruton's tyrosine kinase (Btk) and activation by soluble inositol hexakisphosphate. *eLife* 4.

50. Joseph RE, Min L, & Andreotti AH (2007) The Linker between SH2 and Kinase Domains Positively Regulates Catalysis of the Tec Family Kinases†. *Biochemistry* 46(18):5455-5462.

51. Chopra N, *et al.* (2016) Dynamic Allostery Mediated by a Conserved Tryptophan in the Tec Family Kinases. *PLOS Computational Biology* 12(3):e1004826.

52. Joseph RE, Wales TE, Fulton DB, Engen JR, & Andreotti AH (2017) Achieving a Graded Immune Response: BTK Adopts a Range of Active/Inactive Conformations Dictated by Multiple Interdomain Contacts. *Structure* 25(10):1481-1494.e1484.

53. Joseph RE & Andreotti AH (2009) Conformational snapshots of Tec kinases during signaling. *Immunological Reviews* 228(1):74-92.

54. Márquez JA, *et al.* (2003) Conformation of full-length Bruton tyrosine kinase (Btk) from synchrotron X-ray solution scattering. *The EMBO Journal* 22(18):4616.

55. Readinger JA, *et al.* (2008) Selective targeting of ITK blocks multiple steps of HIV replication. *Proceedings of the National Academy of Sciences of the United States of America* 105(18):6684-6689.

56. Andreotti AH, Schwartzberg PL, Joseph RE, & Berg LJ (2010) T-Cell Signaling Regulated by the Tec Family Kinase, Itk. *Cold Spring Harbor Perspectives in Biology* 2(7).

57. Bradshaw JM (2010) The Src, Syk, and Tec family kinases: Distinct types of molecular switches. *Cellular Signalling* 22(8):1175-1184.

58. Grasis JA & Tsoukas CD (2011) Itk: The Rheostat of the T Cell Response. *Journal of Signal Transduction* 2011:23.

59. Xie Q, Joseph RE, Fulton DB, & Andreotti AH (2013) Substrate Recognition of PLCγ1 via a Specific Docking Surface on Itk. *Journal of molecular biology* 425(4):10.1016/j.jmb.2012.1010.1023.

60. Guendel I, *et al.* (2015) Role of Bruton's tyrosine kinase inhibitors in HIV-1-infected cells. *Journal of NeuroVirology* 21(3):257-275.

61. Tarafdar S, Poe JA, & Smithgall TE (2014) The Accessory Factor Nef Links HIV-1 to Tec/Btk Kinases in an Src Homology 3 Domain-dependent Manner. *Journal of Biological Chemistry* 289(22):15718-15728.

62. Geyer M & Peterlin BM (2001) Domain assembly, surface accessibility and sequence conservation in full length HIV-1 Nef. *FEBS Letters* 496(2–3):91-95.

63. Jia X, *et al.* (2012) Structural basis of evasion of cellular adaptive immunity by HIV-1 Nef. *Nat Struct Mol Biol* 19(7):701-706.

64. Ren X, Park SY, Bonifacino JS, & Hurley JH (2014) How HIV-1 Nef hijacks the AP-2 clathrin adaptor to downregulate CD4. *eLife* 3.

65. Grzesiek S, Stahl SJ, Wingfield PT, & Bax A (1996) The CD4 Determinant for Downregulation by HIV-1 Nef Directly Binds to Nef. Mapping of the Nef Binding Surface by NMR. *Biochemistry* 35(32):10256-10261.

66. Horenkamp FA, *et al.* (2011) Conformation of the Dileucine-Based Sorting Motif in HIV-1 Nef Revealed by Intermolecular Domain Assembly. *Traffic* 12(7):867-877.

67. Poe JA & Smithgall TE (2009) HIV-1 Nef Dimerization Is Required for Nef-Mediated Receptor Downregulation and Viral Replication. *Journal of Molecular Biology* 394(2):329-342.

68. Liu LX, *et al.* (2000) Mutation of a Conserved Residue (D123) Required for Oligomerization of Human Immunodeficiency Virus Type 1 Nef Protein Abolishes Interaction with Human Thioesterase and Results in Impairment of Nef Biological Functions. *Journal of Virology* 74(11):5310-5319.

69. Emert-Sedlak Lori A, *et al.* (2013) Effector Kinase Coupling Enables High-Throughput Screens for Direct HIV-1 Nef Antagonists with Antiretroviral Activity. *Chemistry & Biology* 20(1):82-91.

70. Bentham M, Mazaleyrat S, & Harris M (2006) Role of myristoylation and N-terminal basic residues in membrane association of the human immunodeficiency virus type 1 Nef protein. *Journal of General Virology* 87(3):563-571.

71. Morgan CR, Miglionico BV, & Engen JR (2011) The effects of HIV-1 Nef on human N-myristoyl transferase 1. *Biochemistry* 50(16):3394-3403.

72. Glück JM, Hoffmann S, Koenig BW, & Willbold D (2010) Single Vector System for Efficient N-myristoylation of Recombinant Proteins in E. coli. *PLoS ONE* 5(4):e10081.

73. Boyken SE, Fulton DB, & Andreotti AH (2012) Rescue of the aggregation prone Itk Pleckstrin Homology domain by two mutations derived from the related kinases, Btk and Tec. *Protein Science : A Publication of the Protein Society* 21(9):1288-1297.

74. Severin A, Joseph RE, Boyken S, Fulton DB, & Andreotti AH (2009) Proline isomerization preorganizes the Itk SH2 domain for binding the Itk SH3 domain. *Journal of molecular biology* 387(3):726-743.

75. Mallis RJ, Brazin KN, Fulton DB, & Andreotti AH (2002) Structural characterization of a proline-driven conformational switch within the Itk SH2 domain. *Nat Struct Mol Biol* 9(12):900-905.

76. Boyken SE, *et al.* (2014) A Conserved Isoleucine Maintains the Inactive State of Bruton's Tyrosine Kinase. *Journal of Molecular Biology* 426(21):3656-3669.

77. Lee C-D, *et al.* (2008) An improved SUMO fusion protein system for effective production of native proteins. *Protein Science : A Publication of the Protein Society* 17(7):1241-1248.